

A STRUCTURE AND ASYMPTOTIC PRESERVING SCHEME FOR THE QUASINEUTRAL LIMIT OF THE VLASOV-POISSON SYSTEM

ALAIN BLAUSTEIN¹, GIACOMO DIMARCO², FRANCIS FILBET³ AND MARIE-HÉLÈNE VIGNAL⁴

ABSTRACT. In this work, we propose a new numerical method for the Vlasov–Poisson system that is both asymptotically consistent and stable in the quasineutral regime, *i.e.* when the Debye length is small compared to the characteristic spatial scale of the physical domain. Our approach consists in reformulating the Vlasov–Poisson system as a hyperbolic problem by applying a spectral expansion in the basis of Hermite functions in the velocity space and in designing a structure-preserving scheme for the time and spatial variables. Through this Hermite formulation, we establish a convergence result for the electric field toward its quasineutral limit together with optimal error estimates. Following this path, we then propose a fully discrete numerical method for the Vlasov–Poisson system, inspired by the approach in [6], and rigorously prove that it is uniformly consistent in the quasineutral limit regime. Finally, we present several numerical simulations to illustrate the behavior of the proposed scheme. These results demonstrate the capability of our method to describe quasineutral plasmas and confirm the theoretical findings: stability and asymptotic preservation.

CONTENTS

1. Introduction	2
1.1. The mathematical model and review	2
1.2. Formal quasineutral limit	4
2. Hermite formulation of the quasineutral regime	6
2.1. The Hermite framework	6
2.2. Continuous analysis of the quasineutral regime	7
3. Fully discrete scheme	8
3.1. Phase-space discretization	8
3.2. First order time splitting scheme	9
3.3. Discrete quasineutral limit	10
3.4. Second order time splitting scheme	11
4. Numerical simulations	12
4.1. Near equilibrium	12
4.2. Smooth perturbation of equilibrium	15
4.3. Oscillatory perturbation from equilibrium	16
4.4. Two-stream instability	18
5. Conclusion and perspectives	19
Acknowledgement	21
Appendix A. Proof of Proposition 2.1	21
Appendix B. Proof of Proposition 3.1	29
Appendix C. Proof of Proposition 3.3	32
References	32

2010 *Mathematics Subject Classification.* Primary: 82C40, 35Q83 Secondary: 65N08, 65N35 .

Key words and phrases. Vlasov–Poisson; quasineutral plasma; Hermite spectral method.

¹alain.blaustein@inria.fr, Centre Inria de l’Université de Lille, France.

²giacomo.dimarco@unife.it, Università di Ferrara, Department of Mathematics and Computer Science & Center for Modeling, Computing and Statistics (CMCS), Ferrara, Italy.

³francis.filbet@math.univ-toulouse.fr, Institut de Mathématiques de Toulouse, Université de Toulouse, France.

⁴mhvignal@math.univ-toulouse.fr, Institut de Mathématiques de Toulouse, Université de Toulouse, France.

1. INTRODUCTION

Plasma flows are multiscale problems, involving interactions ranging from microscopic to macroscopic scales [12]. As a result, the numerical simulation of plasmas presents a significant challenge for both the computational physics and the applied mathematics communities. Depending on the physical regime of interest, plasmas are typically described by two main classes of mathematical models: fluid and kinetic models [12, 15]. Fluid models describe the evolution of macroscopic quantities, such as density, temperature, and mean velocity and remain valid when the plasma is close to thermodynamical equilibrium. In contrast, kinetic models detail the time evolution of a distribution function in six-dimensional phase space, representing the probability of a particle occupying a given state at any moment. While these models are able to describe a broader range of physical regimes, they are significantly more computationally demanding.

In this paper, we focus on plasmas far from equilibrium and therefore we adopt a kinetic perspective based on the Vlasov–Poisson system. Specifically, we investigate the challenges related to the quasineutrality, which refers to the assumption that, on macroscopic scales, the net charge density in the plasma is effectively zero. Under this assumption, it is not possible to solve the electric field generated by local charge separations. The macroscopic behavior of the system can be described using asymptotic models, where the electric field is determined by additional constraints on the charge and current densities. However, in some scenarios, quasineutrality and charge imbalances can coexist. This makes challenging the development of numerical methods capable of accurately capturing both effects. Addressing this issue remains an active area of investigation [1, 3, 13, 14, 17, 18, 19].

Here we combine a theoretical analysis of the behavior of the Vlasov-Poisson system in the quasineutral regime with the design of a new numerical method capable of resolving the challenges related to its description. The physical model studied involves several interacting scales, among which the Debye length λ_D and the electron plasma period ω_p^{-1} play a fundamental role:

$$(1.1) \quad \lambda_D := \sqrt{\frac{\varepsilon_0 k_B T_0}{n_0 e^2}}, \quad \omega_p^{-1} := \sqrt{\frac{n_0 e^2}{\varepsilon_0 m}},$$

where n_0 and T_0 are the characteristic density and temperature, e is the elementary charge, ε_0 the vacuum permittivity, k_B the Boltzmann constant, and m the electron mass. The Debye length defines the characteristic scale at which charge imbalances occur, while the electron plasma period represents the characteristic oscillation time associated with electrostatic forces that restore electric neutrality when charge imbalances arise at the Debye length scale [16]. When both the Debye length and the plasma period are small compared to the macroscopic scales of interest, the quasineutral regime holds true and the plasma appears broadly electrically neutral. In the sequel we introduce the details of the model employed.

1.1. The mathematical model and review. Let us first introduce the mathematical model and analyze the different scales involved. The Vlasov-Poisson system provides a kinetic description of a gas constituted of charged particles interacting through a electric field:

$$(1.2) \quad \begin{cases} \frac{\partial f}{\partial t} + v \cdot \nabla_x f + \frac{q}{m} E \cdot \nabla_v f = 0, \\ E = -\nabla_x \phi ; \quad -\varepsilon_0 \Delta_x \phi = q(\rho - \rho_i) ; \quad \rho = \int_{\mathbb{R}^3} f dv. \end{cases}$$

In (1.2), $f(t, x, v)$ is the distribution of electrons over the phase space $(x, v) \in \mathbb{T}^3 \times \mathbb{R}^3$ at time $t \geq 0$. Interactions are taken into account thanks to a coupling between kinetic and Poisson equations (first and second line of (1.2) respectively). The constant q expresses the elementary charge $q = -e < 0$, the scalar function ϕ is the electric potential, while the macroscopic densities of electrons and ions are denoted respectively by $\rho(t, x)$ and $\rho_i(t, x) = \rho_i(x)$. Let us note that in the system (1.2), ions constitute a fixed background, which simplifies the dynamics without omitting the fundamental aspects of the quasineutrality mechanism.

We now introduce the rescaled parameter λ given by

$$\lambda = \frac{\lambda_D}{L} = \left(\frac{\varepsilon_0 k_B T_0}{L^2 e^2 n_0} \right)^{1/2},$$

where L represents the characteristic length at which the physical phenomena are studied, in our case it corresponds to the length of the electric field interactions in plasmas. The quasineutral regime corresponds

to the limit of the Vlasov-Poisson system when $\lambda \rightarrow 0$. This asymptotic limit has been extensively studied in the past by several authors from both the numerical and theoretical points of view. For a theoretical analysis in the context of kinetic and fluid models, see for example [10, 25, 24, 27, 29, 28, 8, 7, 26] and the references therein. The study of the quasineutral limit is often based on reformulation of the Vlasov-Poisson system with respect to the adimensional parameter λ and then in passing to the limit λ going to zero in this rescaled system. Here, we restrict ourselves to the rescaled one dimensional in space and in velocity setting. This leads to the following equations, see in [14, 16] for details,

$$(1.3) \quad \begin{cases} \partial_t f^\lambda + v \partial_x f^\lambda + E^\lambda \partial_v f^\lambda = 0, \\ E^\lambda = -\partial_x \phi^\lambda; -\lambda^2 \partial_x^2 \phi^\lambda = \rho^\lambda - 1; \rho^\lambda(t, x) = \int_{\mathbb{R}} f^\lambda(t, x, v) dv, \end{cases}$$

where $f^\lambda(t, x, v)$, is the distribution at time $t \geq 0$ over the phase-space $(x, v) \in \mathbb{T} \times \mathbb{R}$ and where the density of the ions is assumed to be constant and equal to one everywhere in space. The following condition ensures the uniqueness of ϕ^λ

$$(1.4) \quad \int_{\mathbb{T}} \phi^\lambda(t, x) dx = 0.$$

The model (1.3)-(1.4) possesses the following key properties: conservation of total charge, of total flux (set to 0 for simplicity and without loss of generality) and of the global energy. These read

$$(1.5) \quad \begin{cases} \int_{\mathbb{T}} \rho^\lambda(t, x) dx = \int_{\mathbb{T}} \rho^\lambda(0, x) dx = |\mathbb{T}|, \\ \int_{\mathbb{T}} j^\lambda(t, x) dx = \int_{\mathbb{T}} j^\lambda(0, x) dx = 0, \\ \frac{1}{2} \int_{\mathbb{T}} K^\lambda(t, x) + \lambda^2 |E^\lambda(t, x)|^2 dx = \frac{1}{2} \int_{\mathbb{T}} K^\lambda(0, x) + \lambda^2 |E^\lambda(0, x)|^2 dx, \end{cases}$$

where the flux j^λ , also called the current density, and the kinetic energy $\frac{1}{2}K^\lambda$ are given by

$$(1.6) \quad \begin{cases} j^\lambda(t, x) = \int_{\mathbb{R}} v f^\lambda(t, x, v) dv, \\ K^\lambda(t, x) = \int_{\mathbb{R}} |v|^2 f^\lambda(t, x, v) dv. \end{cases}$$

From a numerical perspective, traditional explicit schemes applied to (1.3) must resolve the microscopic scales related to the small parameter λ^2 to ensure stability and consistency in the limit $\lambda \rightarrow 0$. However, this requirement necessitates extremely small time steps and phase space discretizations in order to remain stable. At the same time, numerical simulations must be performed down to the macroscopic scale to capture meaningful phenomena. This situation creates significant computational challenges and makes these methods impractical for realistic applications. While asymptotic models can be derived to describe macroscopic regimes, additional challenges arise in scenarios where quasineutral and non-quasineutral regions coexist, making simulations particularly difficult.

To address this complexity, domain decomposition approaches or hybrid methods can be employed [11, 20, 22, 23]. However, integrating different models and numerical methods requires to accurately identify interfaces, which remains a challenging task. Therefore, it is crucial to design numerical methods capable of handling multiple regimes simultaneously, without being constrained by small-scale dynamics. The development of schemes that work without such limitations has been the focus of extensive research in the recent years. This is precisely the area in which Asymptotic Preserving (AP) methods have been created, see [31, 21] and [32] for a recent review on the subject. These methods can bypass the above discussed restrictions and automatically achieve transition using consistent discretizations of limiting models as the parameters characterizing microscopic behavior approach zero. The use of Asymptotic Preserving schemes in the context of quasineutrality has been investigated for instance in [14]. The authors proposed a first-order-in-time scheme and a linear stability analysis proving indeed stability for small values of the Debye length of the proposed method. The concept revolved around the reformulation and the consequent discretization of the Poisson equation. This idea was initially introduced in [13] and later used in [3] and [1, 18, 19] or more recently for the Vlasov-Maxwell system [17, 30, 33]. For a general review of numerical methods capturing the quasineutral limit for both kinetic and fluid models, we refer to [16]. In this work, we

adopt an alternative approach that we develop in two parts. First, we study relevant analytical properties of the Vlasov–Poisson system close to the quasineutral limit. Then, we propose a new numerical method based on this theoretical result and perform a discrete counterpart analysis. This allows to highlight the main properties of the scheme such as stability and preservation of the asymptotic state. Unlike previous approaches in the literature [13, 14, 16], our discretization does not rely on reformulating the Poisson equation as an equivalent harmonic oscillator equation. We instead discretize the Poisson equation concurrently with the equations governing the time evolution of the first moments of the distribution function.

In the following section, we first recall the formal limit of the Vlasov–Poisson system as the Debye length approaches zero (Section 1.2). Then, in Section 2, we reformulate the Vlasov–Poisson system as a hyperbolic system with source terms by expanding the distribution function in velocity using a basis of Hermite functions. This reformulation is particularly well-suited for studying the quasineutral limit, as we will demonstrate. Next, we establish a convergence result for the electric field toward its quasineutral limit by explicitly characterizing the oscillatory component of the solution (see Proposition 2.1) and highlighting the impact of the initial conditions on the size of these oscillations. Starting from this formulation, we propose a numerical scheme based on a time-splitting strategy in Section 3. We rigorously prove that the scheme captures the asymptotic behavior of the solution in Section 3.3. In Section 4, we present several numerical simulations to illustrate the behavior of the proposed discretization in relation to the theoretical results of Proposition 2.1, including an analysis of the error estimates. Furthermore, a key aspect of our numerical investigation focuses on scenarios where our analysis does not hold. By studying these cases, we aim to identify the necessary precautions to avoid physically irrelevant results.

1.2. Formal quasineutral limit. Let us now observe that in the regime $\lambda \ll 1$, the second line in (1.3) forces the global neutrality condition expressed by the first line of (1.5) to become a pointwise constraint in x . Thus, one expects the solution f^λ to formally converge to the solution f of the quasineutral system

$$(1.7) \quad \begin{cases} \partial_t f + v \partial_x f + E \partial_v f = 0, \\ \rho(t, x) = 1; \quad \rho(t, x) = \int_{\mathbb{R}} f(t, x, v) dv, \end{cases}$$

where $f(t, x, v)$ is the limiting distribution over the phase-space $(x, v) \in \mathbb{T} \times \mathbb{R}$. The latter system may be confusing at first glance, as the equation on the limiting field E seems to be missing. In fact, E remains fully determined even in (1.7), as it may be interpreted as the Lagrange multiplier associated to the pointwise neutrality constraint from the second line of equations (1.7). Indeed, the quasineutral limit described by system (1.7) together with the conditions (1.5) imposes the limiting electric field and the limiting electric flux to satisfy the following relations

$$(1.8) \quad \begin{cases} j(t, x) = 0, \\ E(t, x) = \partial_x K(t, x), \end{cases}$$

where the kinetic energy $\frac{1}{2}K$ is given by (1.6). Hence, global conservation of the total charge and the total flux in (1.5) both become pointwise constraints in the quasineutral regime, according to the second line of (1.7) and the first line of (1.8) respectively.

Remark 1.1. *Let us observe that (1.8) is obtained multiplying the Vlasov equation (1.7) by $(1, v)^t$ and integrating over $v \in \mathbb{R}$. We then use the pointwise neutrality constraint and total conservation of flux for $j(t, x)$, and both pointwise neutrality and conservation of flux to obtain the expression of the electric field $E(t, x)$.*

Before continuing, we point out that the quasineutral system may not be globally well-posed for all initial data. This was observed in [2] for the related Vlasov–Dirac–Benney system and in [27] near the so-called Penrose unstable profiles for the Vlasov–Poisson system. Indeed, in such cases, small perturbations from the quasineutral state can lead to the development of instabilities in the plasma. In what follows, we restrict our analysis to configurations near Penrose stable profiles. However, in the numerical section, we will simulate both stable and unstable cases to illustrate these phenomena.

One of the key challenges in the numerical analysis and simulation of the quasineutral regime is that the strong convergence of f^λ to f may fail due to the emergence of fast oscillations with period $1/\lambda$ when

$\lambda \ll 1$, see for instance [25, 27, 29, 8]. These oscillations result from the fact that the pointwise neutrality and conservation of flux in (1.7)-(1.8) may not be verified by the non neutral initial distribution $f^\lambda(t=0)$. To uncover these oscillations, we determine their amplitude thanks to formal energy considerations. In particular, we focus on initial configurations with uniformly bounded total energy as $\lambda \ll 1$, that is,

$$\sup_{\lambda>0} \left(\int_{\mathbb{T}} K^\lambda(0, x) + \lambda^2 |E^\lambda(0, x)|^2 dx \right) < +\infty.$$

Since the total energy is conserved by (1.4), this yields for all $t \geq 0$

$$\sup_{\lambda>0} \left(\int_{\mathbb{T}} K^\lambda(t, x) + \lambda^2 |E^\lambda(t, x)|^2 dx \right) < +\infty.$$

In particular, this estimate indicates that E^λ is at most of order $O(\lambda^{-1})$:

$$\sup_{\lambda>0} \left(\lambda \|E^\lambda(t)\|_{L^2(\mathbb{T})} \right) < +\infty; \quad \text{that is,} \quad |E^\lambda(t)| \lesssim \frac{1}{\lambda}, \quad \text{as } \lambda \ll 1,$$

which means that the amplitude of the electric field oscillations is at most of order $O(\lambda^{-1})$. In the following, we restrict our investigation to cases characterized by smaller amplitudes of the electric field, namely

$$(1.9) \quad |E^\lambda(t)| \lesssim \frac{1}{\lambda^\alpha}, \quad \text{for some } 0 \leq \alpha < 1, \quad \text{as } \lambda \ll 1.$$

It is worth mentioning that the analysis of the critical case $\alpha = 1$ significantly differs from the cases where $\alpha < 1$ [25, 27]. We will discuss this critical case in the section devoted to numerical simulations. Now, to identify the period of oscillations, we analyze the coupled system current density j^λ and electric field E^λ , which reads

$$(1.10) \quad \begin{cases} \lambda^2 \partial_t E^\lambda + j^\lambda = 0, \\ \partial_t j^\lambda + \partial_x K^\lambda - \rho^\lambda E^\lambda = 0. \end{cases}$$

This is obtained multiplying the Vlasov equation in (1.3) by $(1, v)^t$, integrating over $v \in \mathbb{R}$ and then substituting the Poisson equation in the continuity equation. We now rewrite the coupled system (1.10) as

$$(1.11) \quad \partial_t \begin{pmatrix} E^\lambda - \partial_x K^\lambda \\ \lambda^{-1} j^\lambda \end{pmatrix} + \frac{1}{\lambda} J \cdot \begin{pmatrix} E^\lambda - \partial_x K^\lambda \\ \lambda^{-1} j^\lambda \end{pmatrix} + \mathbf{R}^\lambda = 0,$$

where the matrix J and the vector \mathbf{R}^λ are given as follows

$$J = \begin{pmatrix} 0 & 1 \\ -1 & 0 \end{pmatrix}, \quad \text{and} \quad \mathbf{R}^\lambda = \begin{pmatrix} \partial_{tx} K^\lambda \\ \lambda^{-1} (1 - \rho^\lambda) E^\lambda \end{pmatrix}.$$

Equation (1.11) shows that the electric field and the flux behave like harmonic oscillators with period $1/\lambda$ up to the source term \mathbf{R}^λ . Indeed, multiplying (1.11) by the matrix $\exp(tJ/\lambda)$ and integrating in time, we obtain the following Duhamel formula

$$\begin{pmatrix} E^\lambda - \partial_x K^\lambda \\ \lambda^{-1} j^\lambda \end{pmatrix} (t) = \exp\left(-\frac{t}{\lambda} J\right) \cdot \begin{pmatrix} E^\lambda - \partial_x K^\lambda \\ \lambda^{-1} j^\lambda \end{pmatrix} (0) - \int_0^t \exp\left(\frac{s-t}{\lambda} J\right) \cdot \mathbf{R}^\lambda(s) ds,$$

for all time $t \geq 0$, where $\exp(tJ)$ is the rotation matrix with angle t :

$$(1.12) \quad \exp(tJ) = \begin{pmatrix} \cos(t) & \sin(t) \\ -\sin(t) & \cos(t) \end{pmatrix}.$$

The difficulty is then to prove that, under the conditions (1.9), the remainder in the Duhamel formula may be neglected in the regime $\lambda \ll 1$ (see also [25, 27, 8, 29]), which yields

$$(1.13) \quad \begin{cases} E^\lambda(t) \underset{\lambda \ll 1}{\simeq} \partial_x K^\lambda(t) + \cos\left(\frac{t}{\lambda}\right) (E^\lambda - \partial_x K^\lambda)(0) - \frac{1}{\lambda} \sin\left(\frac{t}{\lambda}\right) j^\lambda(0), \\ j^\lambda(t) \underset{\lambda \ll 1}{\simeq} 0 + \lambda \sin\left(\frac{t}{\lambda}\right) (E^\lambda - \partial_x K^\lambda)(0) + \cos\left(\frac{t}{\lambda}\right) j^\lambda(0). \end{cases}$$

These formal computations show that the quasi neutral limit (1.8) is satisfied up to fast oscillations of period $1/\lambda$ with amplitude only depending on the initial data $f^\lambda(t=0)$.

To prepare the design and analysis of our numerical method, let us now make this analysis rigorous in the Hermite framework.

2. HERMITE FORMULATION OF THE QUASINEUTRAL REGIME

The Hermite decomposition arises naturally when studying the Vlasov-Poisson system. It corresponds to a moment method tailored with an additional spectral structure and well suited for accurate numerical approximations. We start by recasting (1.3) and (1.7) in the Hermite framework, successively we highlight how quasineutral oscillations naturally uncover in this setting.

2.1. The Hermite framework. We decompose the distribution f^λ and its quasineutral counterpart f into their Hermite coefficients $C^\lambda = (C_k^\lambda)_{k \in \mathbb{N}}$ and $C = (C_k)_{k \in \mathbb{N}}$, that is,

$$(2.1) \quad f^\lambda(t, x, v) = \sum_{k \in \mathbb{N}} C_k^\lambda(t, x) \Psi_k(v) \quad \text{and} \quad f(t, x, v) = \sum_{k \in \mathbb{N}} C_k(t, x) \Psi_k(v),$$

where the basis of Hermite functions $(\Psi_k)_{k \in \mathbb{N}}$ is defined recursively as follows $\Psi_{-1} = 0$, $\Psi_0 = \mathcal{M}$ and

$$(2.2) \quad v \Psi_k(v) = \sqrt{T_0 k} \Psi_{k-1}(v) + \sqrt{T_0(k+1)} \Psi_{k+1}(v), \quad \forall k \geq 0,$$

and where \mathcal{M} denotes the stationary Maxwellian with fixed temperature $T_0 > 0$

$$(2.3) \quad \mathcal{M}(v) = \frac{1}{\sqrt{2\pi T_0}} \exp\left(-\frac{|v|^2}{2T_0}\right).$$

Hermite functions $(\Psi_k)_{k \in \mathbb{N}}$ constitute an orthonormal system for the inverse Gaussian weight:

$$(2.4) \quad \int_{\mathbb{R}} \Psi_k(v) \Psi_l(v) \mathcal{M}^{-1}(v) dv = \delta_{k,l},$$

where $\delta_{k,l}$ denotes the Kronecker symbol ($\delta_{k,l} = 1$ when $k = l$ and $\delta_{k,l} = 0$ otherwise). The decomposition (2.1) may also be interpreted as a moment method, where C_k , $k \geq 0$, stands for the moment of the distribution of order k , appropriately modified in order to satisfy the orthogonality constraint (2.4). In particular, from (2.1) one can easily retrieve the macroscopic quantities associated to f^λ . For example, mass (1.3), current density and kinetic energy (1.6) are given by

$$\rho^\lambda(t, x) = C_0^\lambda(t, x); \quad j^\lambda(t, x) = \sqrt{T_0} C_1^\lambda(t, x); \quad K^\lambda(t, x) = T_0 \left(\sqrt{2} C_2^\lambda + C_0^\lambda \right)(t, x).$$

Thanks to the above decomposition, one can rewrite (1.3) and (1.7) as an infinite hyperbolic system with unknowns $C^\lambda = (C_k^\lambda)_{k \in \mathbb{N}}$ and $C = (C_k)_{k \in \mathbb{N}}$, where the discrete spectral parameter $k \in \mathbb{N}$ now replaces the velocity variable $v \in \mathbb{R}$. More precisely, for each $k \geq 0$, we compute the equation for C_k^λ by multiplying (1.3) with $\Psi_k \mathcal{M}^{-1}$ and integrating over $v \in \mathbb{R}$. We then use (2.2) to compute the contribution of the free transport operator $v \partial_x$ and the following relation to compute the field contribution $\partial_x \phi^\lambda \partial_v$

$$\partial_v (\Psi_k \mathcal{M}^{-1}) = \sqrt{\frac{k}{T_0}} \Psi_{k-1} \mathcal{M}^{-1}, \quad \forall k \geq 0.$$

Finally, the orthogonality property (2.4) is used to close the system of equations. This yields to the following coupled system for the coefficients $C^\lambda = (C_k^\lambda)_{k \in \mathbb{N}}$,

$$(2.5) \quad \begin{cases} \partial_t C_k^\lambda + \sqrt{T_0 k} \partial_x C_{k-1}^\lambda + \sqrt{T_0(k+1)} \partial_x C_{k+1}^\lambda - \sqrt{\frac{k}{T_0}} E^\lambda C_{k-1}^\lambda = 0, & \forall k \in \mathbb{N}, \\ E^\lambda = -\partial_x \phi^\lambda; \quad -\lambda^2 \partial_x^2 \phi^\lambda = C_0^\lambda - 1, \end{cases}$$

where we have set $C_{-1}^\lambda = 0$, whereas the Hermite coefficients $C = (C_k)_{k \in \mathbb{N}}$ related to the asymptotic distribution $f(t, x, v)$ satisfy

$$(2.6) \quad \begin{cases} C_0 = 1, \\ C_1 = 0, \\ \partial_t C_k + \sqrt{T_0 k} \partial_x C_{k-1} + \sqrt{T_0(k+1)} \partial_x C_{k+1} - \sqrt{\frac{k}{T_0}} E C_{k-1} = 0, & \forall k \geq 2, \\ E = \sqrt{2} T_0 \partial_x C_2. \end{cases}$$

In the next section, using the Hermite framework introduced above, we justify the formal computations presented in Section 1.2.

2.2. Continuous analysis of the quasineutral regime. To compute the oscillatory components of $(f^\lambda, \phi^\lambda)$ within the Hermite framework, we first rewrite the Ampère and flux equations (1.10) as

$$(2.7) \quad \lambda^2 \partial_t E^\lambda + \sqrt{T_0} C_1^\lambda = 0, \quad \text{and} \quad \partial_t C_1^\lambda + \sqrt{T_0} \partial_x C_0^\lambda + \sqrt{2T_0} \partial_x C_2^\lambda - \frac{1}{\sqrt{T_0}} E^\lambda C_0^\lambda = 0.$$

Therefore, the system (1.11) takes the form

$$(2.8) \quad \partial_t \begin{pmatrix} E^\lambda - E_{\text{slow}}^\lambda \\ \lambda^{-1} \sqrt{T_0} C_1^\lambda \end{pmatrix} + \frac{1}{\lambda} J \cdot \begin{pmatrix} E^\lambda - E_{\text{slow}}^\lambda \\ \lambda^{-1} \sqrt{T_0} C_1^\lambda \end{pmatrix} + \mathbf{S}^\lambda = 0,$$

where J is defined in (1.11) and \mathbf{S}^λ is given by

$$\mathbf{S}^\lambda = \begin{pmatrix} \sqrt{2} T_0 \partial_t \partial_x C_2^\lambda \\ \lambda^{-1} (T_0 \partial_x C_0^\lambda + E^\lambda (1 - C_0^\lambda)) \end{pmatrix}.$$

The quantity E_{slow}^λ plays the role of the quasineutral electric field and it is defined by

$$E_{\text{slow}}^\lambda := \sqrt{2} T_0 \partial_x C_2^\lambda.$$

In the introduction, we interpreted the system (2.8) as a coupled harmonic oscillator up to a source term \mathbf{S}^λ . To justify this statement, we now analyze the behavior of $E^\lambda - E_{\text{slow}}^\lambda$ and C_1^λ in time. To this aim, we define \mathbf{U}^λ as

$$\mathbf{U}^\lambda(t) := \begin{pmatrix} E^\lambda - E_{\text{slow}}^\lambda \\ \lambda^{-1} \sqrt{T_0} C_1^\lambda \end{pmatrix}(t) - \exp\left(-\frac{t}{\lambda} J\right) \cdot \begin{pmatrix} E^\lambda - E_{\text{slow}}^\lambda \\ \lambda^{-1} \sqrt{T_0} C_1^\lambda \end{pmatrix}(t=0),$$

where $\exp(tJ)$ is the rotation matrix given by (1.12). The vector \mathbf{U}^λ vanishes at $t=0$ while it satisfies the following equation

$$(2.9) \quad \partial_t \mathbf{U}^\lambda + \frac{1}{\lambda} J \cdot \mathbf{U}^\lambda + \mathbf{S}^\lambda = 0.$$

Multiplying (2.9) by $\exp(tJ/\lambda)$ and integrating in time, we obtain the following Duhamel formula

$$(2.10) \quad \mathbf{U}^\lambda(t) = - \int_0^t \exp\left(\frac{s-t}{\lambda} J\right) \cdot \mathbf{S}^\lambda(s) ds, \quad \forall t \geq 0.$$

In Proposition 2.1 below, we prove that if (1.9) is satisfied, the remainder in the former Duhamel formula may be neglected as $\lambda \rightarrow 0$, which leads to the asymptotic expansion (1.13). This result ensures that the field E^λ and the flux C_1^λ converge to the quasineutral limit up to fast oscillations in time.

In the Hermite framework, the formalization of condition (1.9) translates in the following statement: there exists $0 \leq \alpha < 1$ and a final time $T > 0$ such that

$$(2.11) \quad \sup_{0 < \lambda < 1} \left(\lambda^{\alpha-1} \left\| C_1^\lambda(0) \right\|_{W^{r_0+1,4}(\mathbb{T})} + \sup_{t \in [0,T]} \lambda^\alpha \left\| E^\lambda(t) \right\|_{W^{r_0+2,4}(\mathbb{T})} \right) < +\infty,$$

where $r_0 = \lceil 1/(1-\alpha) \rceil$, $\lceil \cdot \rceil$ denotes the upper integer part and where $W^{r_0,4}$ is the Sobolev space of order r_0 based on L^4 . Furthermore, we assume that

$$(2.12) \quad \sup_{0 < \lambda < 1} \sup_{t \in [0,T]} \max_{k \leq 4} \left\| C_k^\lambda(t) \right\|_{W^{r_0+3,4}(\mathbb{T})} < +\infty,$$

meaning that the solution to the Vlasov-Poisson system remains uniformly regular with respect to λ . Under the latter two hypothesis, we are able to prove that the formal expansion (1.13) holds true with optimal convergence rates in λ . To that aim, we define the following quantities

$$(2.13) \quad \begin{cases} \mathcal{E}_0^\lambda(t) := \left\| E^\lambda(t) - E_{\text{slow}}^\lambda(t) - E_{\text{osc}}^\lambda(t) \right\|_{L^2(\mathbb{T})}, \\ \mathcal{E}_1^\lambda(t) := \left\| C_1^\lambda(t) - C_{1,\text{osc}}^\lambda(t) \right\|_{L^2(\mathbb{T})}, \end{cases}$$

where we decompose the electric field into two parts, namely the quasineutral state and its oscillating counterpart, and the same for the current density C_1^λ . These oscillating quantities read

$$(2.14) \quad \begin{cases} E_{\text{osc}}^\lambda(t, x) &:= \cos\left(\frac{t}{\lambda}\right) \left(E^\lambda - E_{\text{slow}}^\lambda\right)(0, x) - \frac{\sqrt{T_0}}{\lambda} \sin\left(\frac{t}{\lambda}\right) C_1^\lambda(0, x), \\ C_{1, \text{osc}}^\lambda(t, x) &:= \cos\left(\frac{t}{\lambda}\right) C_1^\lambda(0, x) + \frac{\lambda}{\sqrt{T_0}} \sin\left(\frac{t}{\lambda}\right) \left(E^\lambda - E_{\text{slow}}^\lambda\right)(0, x). \end{cases}$$

We are now able to prove the following result.

Proposition 2.1. *Consider a family of solutions $(C^\lambda, \phi^\lambda)_{\lambda>0}$ to (2.5) with zero total flux*

$$\int_{\mathbb{T}} C_1^\lambda(t, x) dx = 0,$$

and global mass $|\mathbb{T}|$. Suppose that they satisfy the compatibility assumption (2.11) and the uniform regularity assumption (2.12), for some given final time $T > 0$. Then, for all $t \in [0, T]$, and all $0 < \lambda < 1$, the following bounds hold for the electric field and the flux (E^λ, C_1^λ) :

$$\mathcal{E}_0^\lambda(t) \leq C \lambda^{1-\alpha} \quad \text{and} \quad \mathcal{E}_1^\lambda(t) \leq C \lambda^{2-\alpha},$$

where the constant C only depends on α , T , T_0 , $|\mathbb{T}|$ and the implicit constants in (2.11)-(2.12).

Proof. The proof is postponed in Appendix A. □

Remark 2.2. *It is worth mentioning that our analysis does not cover the critical case $\alpha = 1$. Actually, in this critical case, the limit of f^λ is still valid up to a change of variable, however it is only possible to characterize the convergence of E^λ as*

$$\lambda \left(E^\lambda - E_{\text{osc}}^\lambda\right) \longrightarrow 0, \quad \text{as } \lambda \rightarrow 0,$$

which means that the slow part of E^λ remains not clearly identified, see [25, 27, 29] for details.

3. FULLY DISCRETE SCHEME

In this section, we introduce the numerical scheme used to approximate the Vlasov–Poisson system recast in the Hermite framework (2.5) and we analyze its properties. We begin by discussing the discretization of the phase space $\mathbb{T} \times \mathbb{R}$ in Section 3.1. Then, in Section 3.2, we present a first-order time integration scheme based on operator splitting between linear and nonlinear terms. The theoretical properties of the proposed scheme are then analyzed in Section 3.3. Finally, Section 3.4 is devoted to the extension of the first-order method to higher-order accuracy in time. In particular, we propose a second-order time integration scheme based on Strang splitting, combined with an implicit Runge–Kutta method applied to each substep of the splitting.

3.1. Phase-space discretization. To discretize the phase space domain, we fix a number of Hermite modes $N_H \in \mathbb{N}^*$. Then, we consider the interval (a, b) of \mathbb{R} and for $N_x \in \mathbb{N}^*$, we introduce the set $\mathcal{J} = \{1, \dots, N_x\}$ and a family of control volumes $(K_j)_{j \in \mathcal{J}}$ such that $K_j =]x_{j-1/2}, x_{j+1/2}[$ with x_j the middle of the interval K_j and

$$a = x_{1/2} < x_1 < x_{3/2} < \dots < x_{j-1/2} < x_j < x_{j+1/2} < \dots < x_{N_x} < x_{N_x+1/2} = b.$$

We also define the mesh sizes

$$\begin{cases} \Delta x_j = x_{j+1/2} - x_{j-1/2}, & \text{for } j \in \mathcal{J}, \\ \Delta x_{j+1/2} = x_{j+1} - x_j, & \text{for } 1 \leq j \leq N_x - 1. \end{cases}$$

and the parameter h such that

$$h = \max_{j \in \mathcal{J}} \Delta x_j.$$

We then introduce the discrete operator $\partial_h = (\partial_j)_{j \in \mathcal{J}}$ representing the centered finite volume approximation of ∂_x given by

$$(3.1) \quad \partial_j C = \frac{C_{j+1} - C_{j-1}}{2\Delta x_j}, \quad j \in \mathcal{J},$$

for all $C = (C_j)_{j \in \mathcal{J}}$. The above detailed choices lead to the following semi-discrete system

$$(3.2) \quad \begin{cases} \frac{dC_k}{dt} + \sqrt{k T_0} \partial_h C_{k-1} + \sqrt{(k+1) T_0} \partial_h C_{k+1} - \sqrt{\frac{k}{T_0}} E C_{k-1} = 0, \\ E = -\partial_h \phi; \quad -\lambda^2 \partial_h^2 \phi = C_0 - 1, \end{cases}$$

for $k \in \{0, \dots, N_H\}$ and $C_k = 0$ when $k > N_H$ and $k = -1$. System (3.2) is then completed with the condition

$$\sum_{j \in \mathcal{J}} \Delta x_j \phi_j = 0,$$

ensuring uniqueness of the discrete potential $(\phi_j)_{j \in \mathcal{J}}$.

3.2. First order time splitting scheme. The time discretization is based on a time splitting technique, where the first step consists in solving the Vlasov-Poisson system, linearized around a quasineutral steady state $C^{\text{stat}} = (\delta_{0,k})_{k \in \mathbb{N}}$. The second step, consists in solving the remaining nonlinear part of the system. More precisely, we first rewrite the semi-discrete system (3.2) as

$$(3.3) \quad \frac{dC_k}{dt} + \mathcal{L}_k C + \mathcal{B}_k(C) = 0,$$

for each $k \in \{0, \dots, N_H\}$. We separate the contribution of the linear operator $\mathcal{L} = (\mathcal{L}_k)_{0 \leq k \leq N_H}$ from that of the nonlinear operator $\mathcal{B} = (\mathcal{B}_k)_{0 \leq k \leq N_H}$. The first discrete operator is defined for the modes $C = (C_k)_{0 \leq k \leq N_H}$ as

$$\mathcal{L}_k C = \sqrt{k T_0} \partial_h C_{k-1} + \sqrt{(k+1) T_0} \partial_h C_{k+1}, \quad \text{for } k \neq 1,$$

with $C_k = 0$ when $k > N_H$ and $k = -1$ and

$$\mathcal{L}_1 C = \sqrt{T_0} \partial_h C_0 + \sqrt{2 T_0} \partial_h C_2 - \frac{1}{\sqrt{T_0}} E, \quad \text{with } E = -\partial_h \phi, \quad \text{and } -\lambda^2 \partial_h^2 \phi = C_0 - 1.$$

The second nonlinear operator $\mathcal{B} = (\mathcal{B}_k)_{0 \leq k \leq N_H}$ is defined by

$$\begin{cases} \mathcal{B}_0(C) = 0, \\ \mathcal{B}_k(C) = -\sqrt{\frac{k}{T_0}} E (C_{k-1} - \delta_{1,k}), \quad \text{if } k \geq 1, \\ E = -\partial_h \phi, \quad \text{and } -\lambda^2 \partial_h^2 \phi = C_0 - 1, \end{cases}$$

where $\delta_{1,k}$ denotes the Kronecker symbol. We then fix a time step $\Delta t > 0$, set $t^n = n \Delta t$ with $n \in \mathbb{N}$, and solve first the linear part on $[t^n, t^{n+1}]$ with a first order fully implicit Euler scheme. This yields the following linear system to invert

$$(3.4) \quad \begin{cases} \frac{C_1^{(1)} - C_1^n}{\Delta t} + \sqrt{T_0} \partial_h C_0^{(1)} + \sqrt{2 T_0} \partial_h C_2^{(1)} - \frac{1}{\sqrt{T_0}} E^{(1)} = 0, \\ \frac{C_k^{(1)} - C_k^n}{\Delta t} + \sqrt{k T_0} \partial_h C_{k-1}^{(1)} + \sqrt{(k+1) T_0} \partial_h C_{k+1}^{(1)} = 0, \quad \text{for } k \neq 1, \\ E^{(1)} = -\partial_h \phi^{(1)}; \quad -\lambda^2 \partial_h^2 \phi^{(1)} = C_0^{(1)} - 1, \end{cases}$$

where $C^{(1)}$ indicates the solution obtained after this first splitting-step for $k \in \{0, \dots, N_H\}$ and, as before, with $C_k^{(1)} = 0$ when $k > N_H$ and $k = -1$. To the above system (3.4), we add the following uniqueness condition

$$\sum_{j \in \mathcal{J}} \Delta x_j \phi_j^{(1)} = 0.$$

Let us observe that equations (3.4) can be recast in matrix-vector form, where the coefficients of the unknowns are independent of the time index n . Therefore, one can perform an LU factorization of the system at $n = 0$ and store the resulting LU factors to be reused for all $n \geq 0$ improving computational

efficiency. We now focus on the second part of the splitting which involves the nonlinear operator \mathcal{B} . This corresponds to

$$\begin{cases} \frac{dC_k}{dt} + \mathcal{B}_k(C) = 0, \\ C(t^n) = C^{(1)}. \end{cases}$$

We approximate the above system by using again a fully implicit Euler scheme. This reads

$$(3.5) \quad \begin{cases} C_0^{n+1} = C_0^{(1)}, \\ E^{n+1} = E^{(1)}, \\ \frac{C_k^{n+1} - C_k^{(1)}}{\Delta t} - \sqrt{\frac{k}{T_0}} E^{n+1} (C_{k-1}^{n+1} - \delta_{k,1}) = 0, \quad \text{if } k \geq 1, \end{cases}$$

for $k \in \{0, \dots, N_H\}$ and $C_k^{n+1} = 0$ when $k > N_H$. Observe that since the electric field $E^{(1)}$ and the density $C_0^{(1)}$ do not change during this second step, the latter system is trivially invertible and hence does not require any particular linear solver.

The novelty of this approach lies in discretizing the Poisson equation simultaneously with the equations governing the Hermite coefficients $(C_k)_{0 \leq k \leq N}$, as in [6, 4]. Let us observe that the strategy above discussed differs from other recent approaches that reformulate the Poisson equation as a harmonic oscillator-type equation for the potential ϕ , and then build a numerical scheme based on that reformulation (see, for instance, [13, 3, 1, 18, 19, 14, 17]). In contrast, our method retains the original structure of the Vlasov–Poisson system. However, as we explain later in Proposition 3.3, it is still possible to recover a harmonic oscillator formulation for the electric potential from the system (3.4)–(3.5) as done in previous works. Ultimately, we emphasize the importance of solving the coefficients (C_0, C_1, ϕ) in a completely implicit manner, as they exhibit fast oscillations in the quasineutral regime.

3.3. Discrete quasineutral limit. In this section, we investigate the theoretical properties of the numerical method (3.4)–(3.5). In Proposition 3.1, we show that the proposed scheme provides a consistent discretization of the quasineutral limit for a fixed time step Δt . In addition to this result, in Proposition 3.3, we demonstrate that the proposed numerical method naturally encodes the harmonic oscillator reformulation of the Poisson equation.

We start by proving that a discrete counterpart of Proposition 2.1 holds true with however a fundamental difference: the numerical scheme (3.4)–(3.5) filters out the oscillations when the parameter λ tends to 0 and Δt is fixed. This is a consequence of the dissipative nature of the implicit scheme. More precisely, we prove that, for a fixed time step and under a discrete version of the assumption (2.11), the numerical method (3.4)–(3.5) consistently approximates the quasineutral limit in the sense that:

$$E^n \underset{\lambda \rightarrow 0}{=} \sqrt{2} T_0 \partial_h C_2^n + O(\lambda), \quad \text{and} \quad C_1^n \underset{\lambda \rightarrow 0}{=} O(\lambda).$$

To state our result, we use the discrete L^2 and H^r norms of $C = (C_j)_{j \in \mathcal{J}}$, defined as

$$\|C\|_{l^2(\mathcal{J})}^2 = \sum_{j \in \mathcal{J}} |C_j|^2 \Delta x_j, \quad \text{and} \quad \|C\|_{h^r(\mathcal{J})}^2 = \sum_{0 \leq s \leq r} \|\partial_h^s C\|_{l^2(\mathcal{J})}^2.$$

We also introduce the discrete analog of \mathcal{E}_0 and \mathcal{E}_1 of Proposition 2.1, in which we remove the oscillatory part of the solution. They read

$$(3.6) \quad \begin{cases} \mathcal{E}_0^n := \|E^n - \sqrt{2} T_0 \partial_h C_2^n\|_{L^2(\mathcal{J})}, \\ \mathcal{E}_1^n := \|C_1^n\|_{h^1(\mathcal{J})}. \end{cases}$$

We are now ready to prove the following result.

Proposition 3.1. *Let us consider a fixed $\Delta t > 0$ and a solution $(C^n, \phi^n)_{n \geq 0}$ to (3.4)–(3.5) with zero total flux and with total mass $|b - a|$, that is,*

$$(3.7) \quad \sum_{j \in \mathcal{J}} C_{1,j}^0 \Delta x_j = 0, \quad \text{and} \quad \sum_{j \in \mathcal{J}} C_{0,j}^0 \Delta x_j = |b - a|.$$

Suppose furthermore that $(C^n, \phi^n)_{n \geq 0}$ satisfies the discrete analog of (2.11) with $\alpha = 1$, that is,

$$(3.8) \quad \sup_{\lambda > 0} \sup_{0 \leq n \leq T/\Delta t} \left(\|C_1^n\|_{h^1(\mathcal{J})} + \lambda \|E^n\|_{h^3(\mathcal{J})} \right) < +\infty,$$

for some given final time $T > 0$, and that the discrete analog of (2.12) is satisfied, that is,

$$(3.9) \quad \sup_{0 < \lambda} \sup_{0 \leq n \leq T/\Delta t} \sum_{2 \leq k \leq N_H} \|C_k^n\|_{h^2(\mathcal{J})}^2 < +\infty.$$

In addition, suppose that the spatial mesh satisfies the following regularity constraint

$$(3.10) \quad \sup_{\lambda > 0} \sup_{(i,j) \in \mathcal{J}^2} \Delta x_i / \Delta x_j < +\infty.$$

Then, we have for all $\lambda > 0$

$$(3.11) \quad \sup_{1 \leq n \leq T/\Delta t} \mathcal{E}_0^n \leq C\lambda, \quad \text{and} \quad \sup_{2 \leq n \leq T/\Delta t} \mathcal{E}_1^n \leq C\lambda,$$

where $C > 0$ depends on Δt and on the implicit constants in (3.8)-(3.9) and (3.10). Furthermore, the constant C is uniform with respect to λ and the phase-space discretization parameters $h > 0$ and $N_H \geq 2$.

The proof is detailed in Appendix B. The key point consists in proving that for $\Delta t > 0$, the scheme (3.4)-(3.5) filters the fast oscillations of E^n and C_1^n around the quasineutral state. This permits to show that the amplitude of E^n and C_1^n , prescribed by (3.8), are reduced by a factor λ for all $n \geq 1$. The main mathematical difficulty of the proof arises in the analysis of the nonlinear step (3.5). This requires the use of the discrete Sobolev injection $h^1(\mathcal{J}) \hookrightarrow l^\infty(\mathcal{J})$.

Remark 3.2. We emphasize that our result remains valid in the critical case $\alpha = 1$, which was not treated in the continuous setting. In this critical case, the work [25] shows that f^λ converges to the quasineutral limit up to an oscillating change of variable in velocity. This means that the numerical method filters this change of variable and the numerical solution converges to the quasineutral limit directly.

As already mentioned, recently proposed numerical methods addressing the quasineutrality issue uses to reformulate the Poisson equation as a harmonic oscillator equation. In the continuous Hermite framework, this reformulated Poisson equation can be derived by differentiating the Poisson equation (second line of (2.5)) twice in time and substituting C_0^λ and C_1^λ using their corresponding evolution equations (first line of (2.5) for $k = 0$ and 1). These computations lead to the so-called reformulated Poisson equation:

$$(3.12) \quad \lambda^2 \partial_t^2 (\partial_x E^\lambda) + \partial_x (C_0^\lambda E^\lambda) = \partial_x^2 (\sqrt{2} T_0 C_2^\lambda + T_0 C_0^\lambda).$$

It is then natural to ask whether an analogous discrete reformulated Poisson equation from the proposed scheme can be obtained in our setting. This is the object of the following result.

Proposition 3.3. Let $(C^n)_{n \geq 0}$ be a solution to (3.4)-(3.5) with $E = -\partial_h \phi$. Then, the following reformulated discrete Poisson equation for all $n \geq 1$ holds true:

$$(3.13) \quad \begin{aligned} & \lambda^2 \frac{\partial_h E^{n+1} - 2 \partial_h E^n + \partial_h E^{n-1}}{\Delta t^2} + \partial_h \left(E^{n+1} C_0^{n+1} \right) \\ & = \partial_h^2 \left(\sqrt{2} T_0 C_2^{(1,n+1)} + T_0 C_0^{n+1} \right) + \lambda^2 \Delta t \partial_h \left(\frac{E^{n+1} \partial_h E^{n+1} - E^n \partial_h E^n}{\Delta t} \right), \end{aligned}$$

where $C_2^{(1,n+1)}$ corresponds to the Hermite coefficient $C_2^{(1)}$ computed during the step (3.4) of the time splitting scheme to get $(C_k^{n+1})_{k \geq 0}$ from $(C_k^n)_{k \geq 0}$.

The proof is postponed in Appendix C.

3.4. Second order time splitting scheme. In this section, we extend the first-order time method described in (3.4)-(3.5) to a second-order discretization. To this end, observe that each step of the time-splitting scheme (3.4)-(3.5) consists of a first-order implicit method. Therefore, this approach can be generalized to higher-order schemes by employing existing Runge-Kutta techniques [9, 34] and high-order splitting schemes. In particular, we apply a second-order time-splitting strategy (Strang splitting), combined with a second-order stiffly accurate implicit Runge-Kutta method. Thus, given the equation

$$(3.14) \quad \frac{dC_k}{dt} + \mathcal{L}_k C + \mathcal{B}_k(C) = 0,$$

for all coefficients $k \in \{0, \dots, N_H\}$ of the Hermite expansion, we proceed as follows. For each time step starting from C^n , we first solve the linear part on half time step $\Delta t/2$ by taking as initial data $C^{(0)} = C^n$:

$$\frac{dC_k}{dt} + \mathcal{L}_k C = 0,$$

for all coefficients $k \in \{0, \dots, N_H\}$. We set $C^{(1)}$ the solution obtained after this half time step and then we solve the nonlinear part on a full time step Δt using $C^{(1)}$ as initial data. This reads

$$\frac{dC_k}{dt} + \mathcal{B}_k(C) = 0.$$

Finally, by setting $C^{(2)}$ the solution obtained after this second step as a new initial data, we conclude the splitting procedure by solving the linear part on another half time step $\Delta t/2$:

$$\frac{dC_k}{dt} + \mathcal{L}_k C = 0.$$

This gives $C^{(3)} = C^{n+1}$ The solution at time t^{n+1} . Moreover, each of the substeps above is solved using a second-order, fully implicit, stiffly accurate Runge–Kutta scheme, defined as follows:

$$\begin{cases} K_1 = \mathcal{F} \left(C^{(i)} - \gamma \overline{\Delta t} K_1 \right), \\ K_2 = \mathcal{F} \left(C^{(i)} - (1 - \gamma) \overline{\Delta t} K_1 - \gamma \overline{\Delta t} K_2 \right), \\ C^{(i+1)} = C^{(i)} - (1 - \gamma) \overline{\Delta t} K_1 - \gamma \overline{\Delta t} K_2, \end{cases}$$

where $\mathcal{F} \in \{\mathcal{L}, \mathcal{B}\}$, $\gamma = 1 - \frac{1}{\sqrt{2}}$, and $\overline{\Delta t}$ denotes Δt in the case of the nonlinear component and $\Delta t/2$ in the case of the two half-steps for the linear component. Finally the superscripts (i) and $(i+1)$ indicate respectively the value of the Hermite coefficients at the beginning and at the end of the Strang splitting substep.

4. NUMERICAL SIMULATIONS

The numerical experiments are conducted using the second order method presented in the previous Section 3.4. The temperature T_0 is fixed to $T_0 = 1$ for all tests, while the other numerical parameters are chosen based on the specific test case in order to accurately capture the physical phenomena under investigation.

4.1. Near equilibrium. We first consider an initial distribution for the Vlasov–Poisson system (1.3), consisting of a perturbation from a global Maxwellian state of order $\delta \lambda^{2-\alpha}$, with $\alpha \in [0, 1)$, given by

$$(4.1) \quad f_{\text{in}}^\lambda(x, v) = \frac{1}{\sqrt{2\pi}} \left(1 + \delta \lambda^{2-\alpha} \cos(k_x x) \right) \exp\left(-\frac{|v|^2}{2}\right).$$

The spatial domain is $x \in [-10, 10]$, the frequency $k_x = \pi/10$ while we fix the size of the perturbation to $\delta = 0.1$. For this initial data and when $\alpha \in [0, 1)$, it has been shown in [27] that in the limit $\lambda \rightarrow 0$, the solution f^λ to (1.3) converges toward f^0 defined as

$$(4.2) \quad f^0(v) = \frac{1}{\sqrt{2\pi}} \exp\left(-\frac{|v|^2}{2}\right),$$

whereas E^λ weakly converges to $E^0 = 0$, which corresponds to the stationary solution of the quasineutral model (1.7).

First, a reference solution is computed to assess the numerical order of convergence of the quantities \mathcal{E}_0^λ and \mathcal{E}_1^λ , defined in (2.13)-(2.14), describing the oscillatory components of the electric field E^λ and C_1^λ , respectively. This solution uses $N_H = 128$ Hermite modes, $N_x = 2048$ mesh points in the physical space and $\Delta t = 10^{-4}$ is chosen to resolve the smallest value of the Debye length considered in this test, that is, $\lambda = 10^{-2}$.

In Figure 4.1-(a) the time evolution of the rescaled potential energy

$$\frac{1}{2} \sum_{j \in \mathcal{J}} \Delta x_j |E_j^n|^2,$$

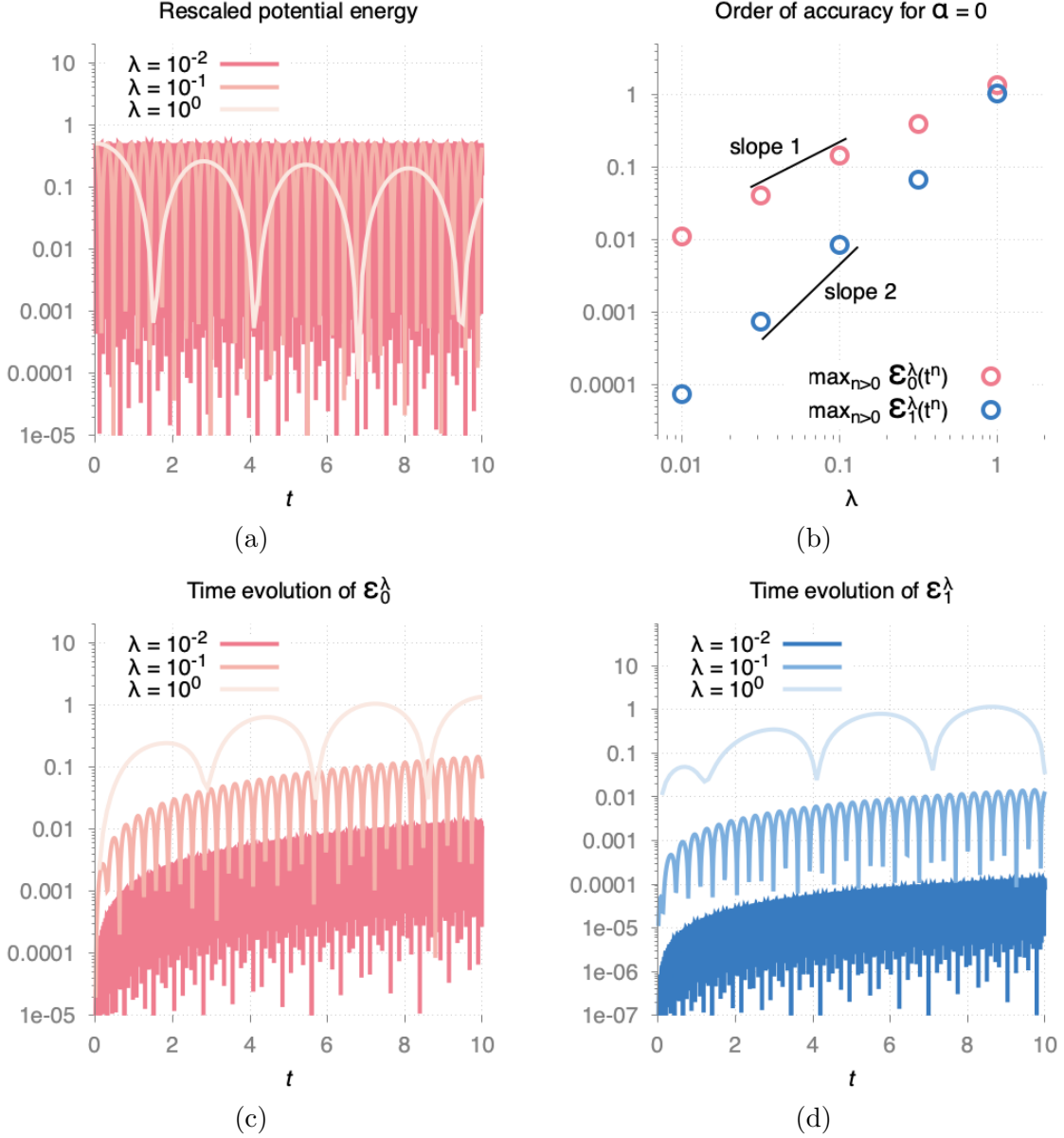


FIGURE 4.1. **Near equilibrium test case with $\alpha = 0$** : (a) time evolution of the rescaled potential energy $\frac{1}{2} \sum_{j \in \mathcal{J}} \Delta x_j |E_j^n|^2$; (b) order of convergence for $\max_{n \geq 0} \mathcal{E}_0^\lambda(t^n)$ and $\max_{n \geq 0} \mathcal{E}_1^\lambda(t^n)$; (c) time evolution of $\mathcal{E}_0^\lambda(t)$ and (d) time evolution of $\mathcal{E}_1^\lambda(t)$, as defined in (2.13)-(2.14), for different values of λ .

is shown in the case $\alpha = 0$. The oscillatory nature of the electric field with a frequency inversely proportional to λ appears clearly. Figure 4.1-(b) represents the quantities

$$\max_{n \geq 0} \mathcal{E}_0^\lambda(t^n) \quad \text{and} \quad \max_{n \geq 0} \mathcal{E}_1^\lambda(t^n),$$

defined in (2.13)-(2.14) for different values of λ . This illustrates Proposition 2.1, which established first and second order of convergence for \mathcal{E}_0^λ and \mathcal{E}_1^λ respectively. Moreover, these figures exhibit that E^λ converges to its quasineutral limit E^0 up to the fast oscillations in time of E_{osc}^λ which are explicitly given in terms of the initial condition by (2.14).

Figure 4.2 displays the same quantities as Figure 4.1, in the case of $\alpha = 1/2$. We observe that, as predicted by the theory, the amplitude of the electric field is now of order $O(\lambda^{-1/2})$ as λ approaches zero (Figure 4.2-(a)). Our numerical outcomes correspond to the theoretical results of Proposition 2.1 regarding the oscillation frequency in time and the order of convergence of the quantity \mathcal{E}_0^λ and \mathcal{E}_1^λ (Figure 4.2-(b)). Let us observe that, while the norm of E^λ grows as $\lambda \rightarrow 0$, the electric field E^λ strongly converges to its quasineutral limit E^0 up to explicitly known fast oscillations in time.

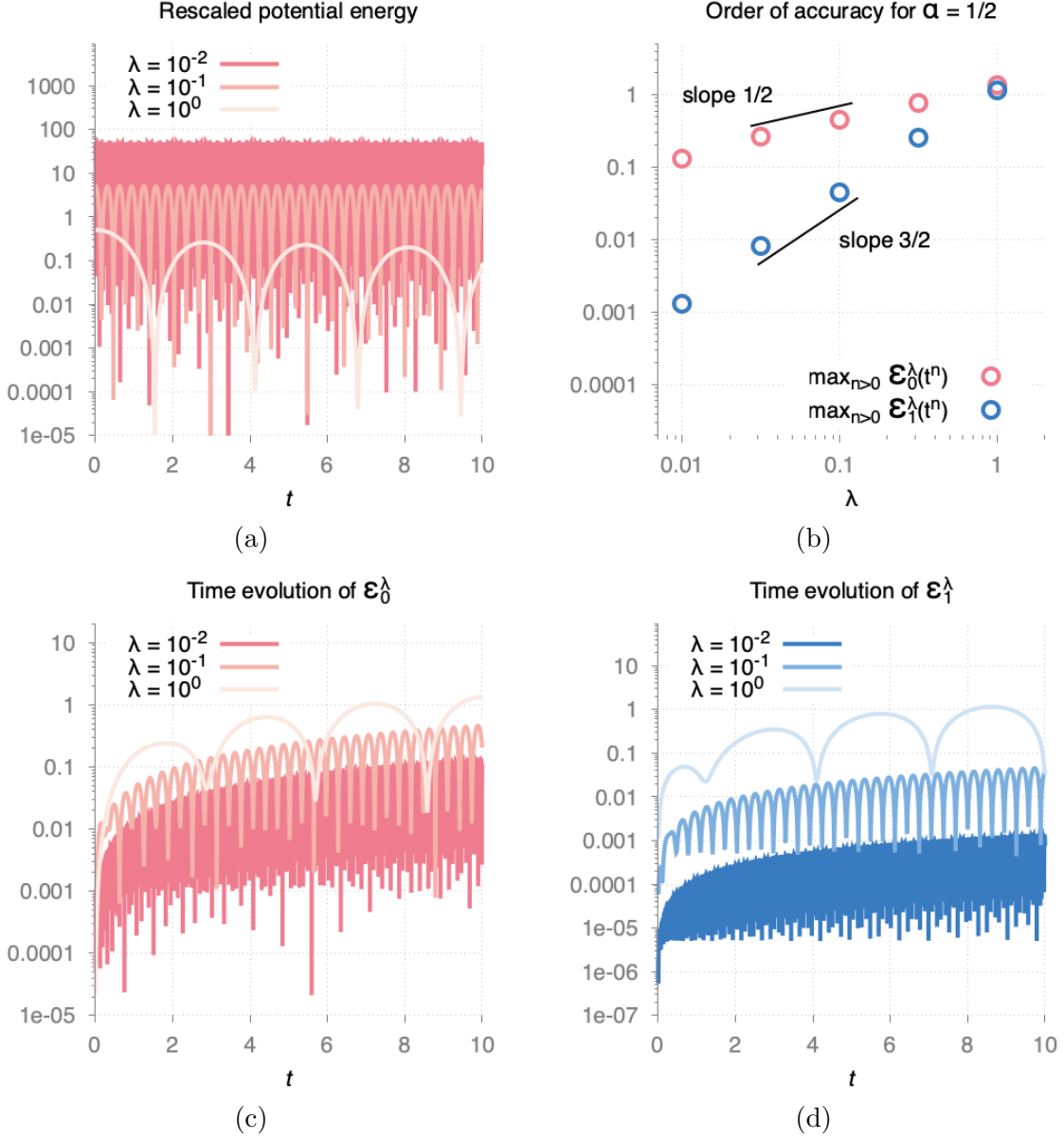


FIGURE 4.2. **Near equilibrium test case with $\alpha = 1/2$** : (a) time evolution of the rescaled potential energy $\frac{1}{2} \sum_{j \in \mathcal{J}} \Delta x_j |E_j^n|^2$; (b) order of convergence for $\max_{n \geq 0} \mathcal{E}_0^\lambda(t^n)$ and $\max_{n \geq 0} \mathcal{E}_1^\lambda(t^n)$; (c) time evolution of $\mathcal{E}_0^\lambda(t)$ and (d) time evolution of $\mathcal{E}_1^\lambda(t)$, as defined in (2.13)-(2.14), for different values of λ .

We then consider the case $\alpha = 1$. This situation is not in the scope of our theoretical analysis but it allows us to test its range of validity. The results are shown in Figure 4.3. The amplitude of the electric field is now of order $O(\lambda^{-1})$ while $\max_{n \geq 0} \mathcal{E}_0^\lambda(t^n)$ no longer converges to zero as $\lambda \rightarrow 0$ (Figure 4.3-(b) and (c)). This is in line with theoretical investigations [25, 27, 29], which show that $\lambda \mathcal{E}_0^\lambda \rightarrow 0$. In contrast, the quantity \mathcal{E}_1^λ remains of the order of λ (Figure 4.3-(b) and (d)). These results suggest that Proposition 2.1 may remain true with $\alpha = 1$.

Finally, we investigate the behavior of our numerical scheme when the time step Δt and the space mesh size are fixed while the quasineutral parameter λ tends to zero. The aim is to study the ability of the scheme to capture the asymptotic behavior of the solution and to illustrate the asymptotic preserving property shown in Proposition 3.1. The numerical parameters are $\Delta t = 0.2$, $N_x = 64$ and $N_H = 128$ and Figure 4.4 displays the numerical results. For $\alpha = 0$ and $\alpha = 1/2$, the time evolution of the potential energy gives results in line with the theoretical findings even for a large time step $\Delta t = 0.2$, both in terms of amplitude and frequency of oscillations (Figure 4.4-(a) and (b)). However, when λ becomes smaller ($\lambda = 10^{-2}$ and 10^{-3}), these discretization parameters are no longer sufficient to describe the small time scales. Hence, the electric field converges toward the expected weak limit. For the case $\alpha = 1$, where the results of Proposition

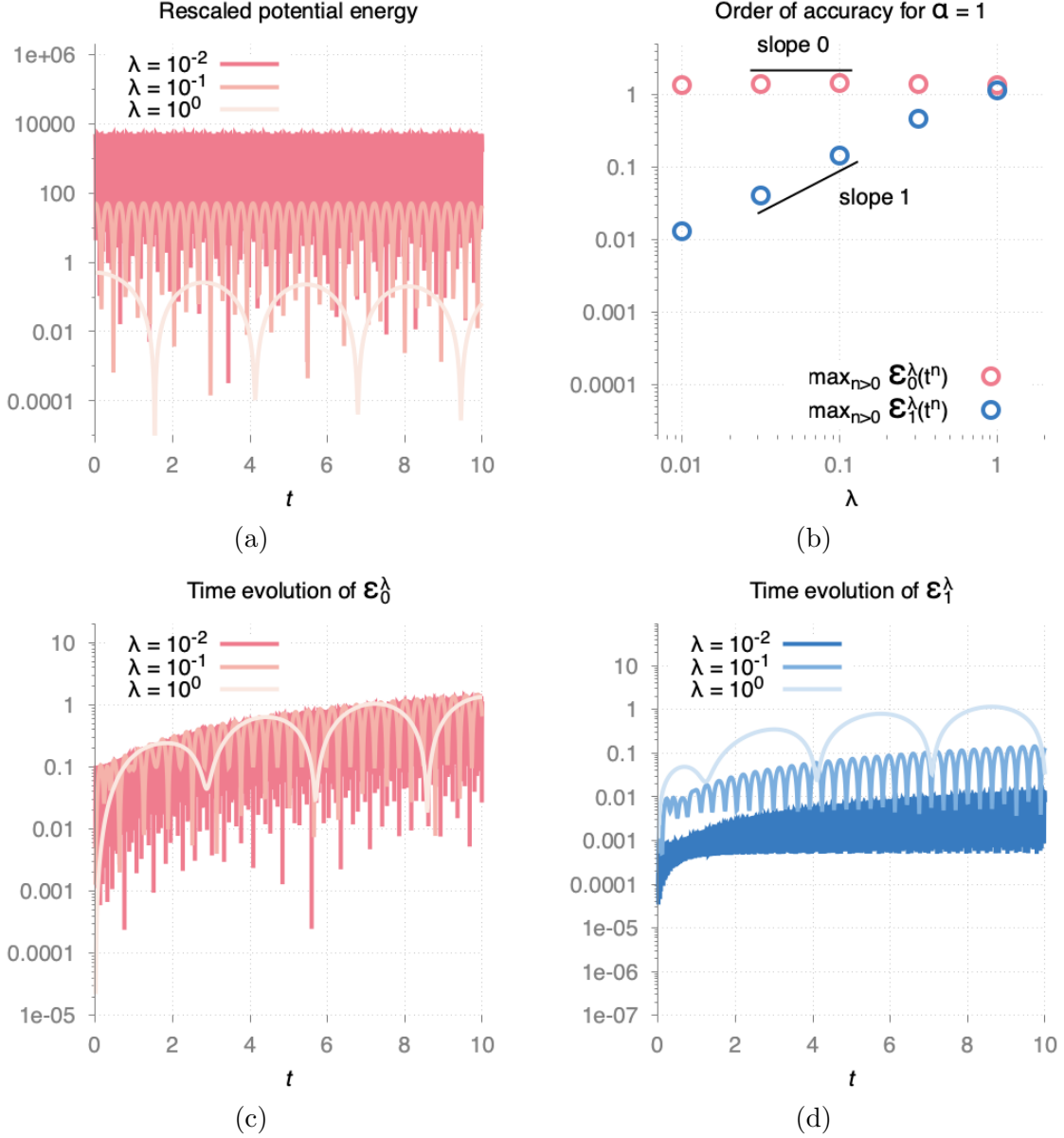


FIGURE 4.3. **Near equilibrium test case with $\alpha = 1$** : (a) time evolution of the rescaled potential energy $\frac{1}{2} \sum_{j \in \mathcal{J}} \Delta x_j |E_j^n|^2$; (b) order of convergence for $\max_{n \geq 0} \mathcal{E}_0^\lambda(t^n)$ and $\max_{n \geq 0} \mathcal{E}_1^\lambda(t^n)$; (c) time evolution of $\mathcal{E}_0^\lambda(t)$ and (d) time evolution of $\mathcal{E}_1^\lambda(t)$, as defined in (2.13)-(2.14), for different values of λ .

2.1 are no longer valid, we observe that, for $\lambda = 10^{-1}$ and 10^{-2} (Figure 4.4(c)), the numerical solution becomes unstable and blows-up. This demonstrates that in such cases, time step and spatial mesh need to be refined to obtain stable results. This lack of uniform stability should not be interpreted as a limit of the scheme, since in this case Proposition 3.1 does not apply and the amplitude of the electric field is proportional to λ^{-1} during the first time steps. Hence, the nonlinear step (3.5) in our time splitting scheme becomes unstable for such a configuration. However, it is interesting to notice that, for $\lambda = 10^{-3}$ and $\Delta t = 0.2$, the scheme regains stability and the rescaled potential energy is instantaneously damped, which means that the electric field E^λ converges to zero.

4.2. Smooth perturbation of equilibrium. We now consider an initial distribution with non homogeneous temperature driven by a perturbation of order $O(1)$ as $\lambda \rightarrow 0$. This reads

$$(4.3) \quad f_{\text{in}}(x, v) = \frac{1}{\sqrt{2\pi T_{\text{in}}(x)}} \exp\left(-\frac{|v|^2}{2T_{\text{in}}(x)}\right),$$

with $x \in [-10, 10]$, frequency $k_x = \pi/10$ and T_{in} given by

$$T_{\text{in}}(x) = 1 + \delta \cos(k_x x).$$

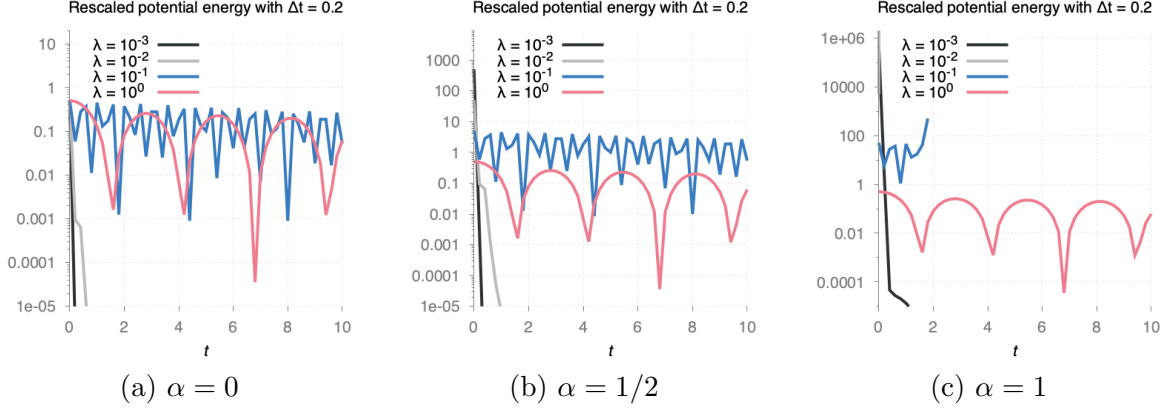


FIGURE 4.4. **Near equilibrium test case.** Time evolution of the rescaled potential energy $\frac{1}{2} \sum_{j \in \mathcal{J}} \Delta x_j |E_j^n|^2$ with $\Delta t = 0.2$, $N_x = 64$ and $N_H = 128$ for different λ : (a) $\alpha = 0$; (b) $\alpha = 1/2$; (c) $\alpha = 1$.

This gives for the density and the flux the following relations

$$\rho_{\text{in}}(x) = \int_{\mathbb{R}} f_{\text{in}}(x, v) dv = 1 \quad \text{and} \quad j_{\text{in}}(x) = \int_{\mathbb{R}} f_{\text{in}}(x, v) v dv = 0, \quad \forall x \in (-10, 10).$$

In this situation, the quasineutral model (1.7) has a non trivial slow dynamics in time that we wish to describe using the proposed numerical approximation.

The reference solution is obtained using the second order scheme provided in Section 3.4 with a fine mesh, $N_H = 2000$, $N_x = 1000$ and $\Delta t = 10^{-3}$, which permits to describe both the fast and the slow scales for different values of the Debye length, namely $\lambda \in \{1, 0.3, 0.1, 0.03\}$. The time evolution of the L^2 norm of the electric field E^λ and the slow component $E_{\text{slow}}^\lambda = \sqrt{2} \partial_x C_2^\lambda$ are shown in Figure 4.5 and in Figure 4.6 respectively (red curves). When $\lambda = 1$, a damping of the electric field is observed as opposite to the case $\lambda \ll 1$, where the electric field oscillates with a frequency inversely proportional to the Debye length λ . At the same time, the slow component E_{slow}^λ is first strongly damped, then it oscillates slowly (independently of λ) and finally, when its amplitude is in order of $\delta \lambda^2$, it starts to oscillate rapidly with a frequency inversely proportional to λ . The observed results stay in good agreement with the analytical investigations of [25, 29, 8].

In Figures 4.5 and 4.6, the accuracy and robustness of the second order scheme for a wide range of λ is measured using $N_x = 100$, $\Delta t = 0.2$, $N_H = 400$ with different values of the Debye length $\lambda \in \{1, 10^{-1}, 10^{-2}, 10^{-3}\}$. The numerical results show both the time evolution of the L^2 norm of the electric field E^λ and its slow counterpart E_{slow}^λ .

When λ and Δt are of the same order, the discrete system is not stiff and a coarse mesh allows to describe precisely the time oscillations as seen in Figures 4.5 and 4.6 (a)-(b). When λ becomes smaller, the time step $\Delta t = 0.2$ is too large to provide a good approximation of the fast scales as one can notice in Figures 4.5 and 4.6 (c)-(d). However, from Figure 4.6-(c), one can observe that when the norm of E_{slow}^λ is larger than the threshold $\delta \lambda^2$, the numerical scheme is still able to describe correctly the slow scale dynamics of E_{slow}^λ . When $\lambda = 3 \cdot 10^{-2}$, the numerical method eliminates the fast physical oscillations and projects the solution on the quasineutral slow dynamics limit, see Figures 4.5-(d) and 4.6-(d)). It is worth mentioning that when $\lambda \rightarrow 0$, the numerical scheme still captures the slow dynamics with $\Delta t = 0.2$, which illustrates its asymptotic preserving property (see Figure 4.7).

In summary, the numerical results definitively show the stability and consistency of the numerical scheme (3.4)-(3.5) in the quasineutral regime, without a prohibitive computational cost. A trade-off inherent of this approach is the filtering of high-frequency oscillations.

4.3. Oscillatory perturbation from equilibrium. We now consider an oscillatory initial distribution by modifying the previous one. More precisely, we choose f_{in} as

$$(4.4) \quad f_{\text{in}}(x, v) = \frac{1}{\sqrt{2\pi T_{\text{in}}(x)}} (1 + \delta \cos(k_x x) \sin(3\pi v)) \exp\left(-\frac{|v|^2}{2T_{\text{in}}(x)}\right),$$

with $\delta = 0.05$, $x \in [-10, 10]$, $k_x = \pi/10$ and T_{in} given by

$$T_{\text{in}}(x) = 1 + \delta \cos(k_x x).$$

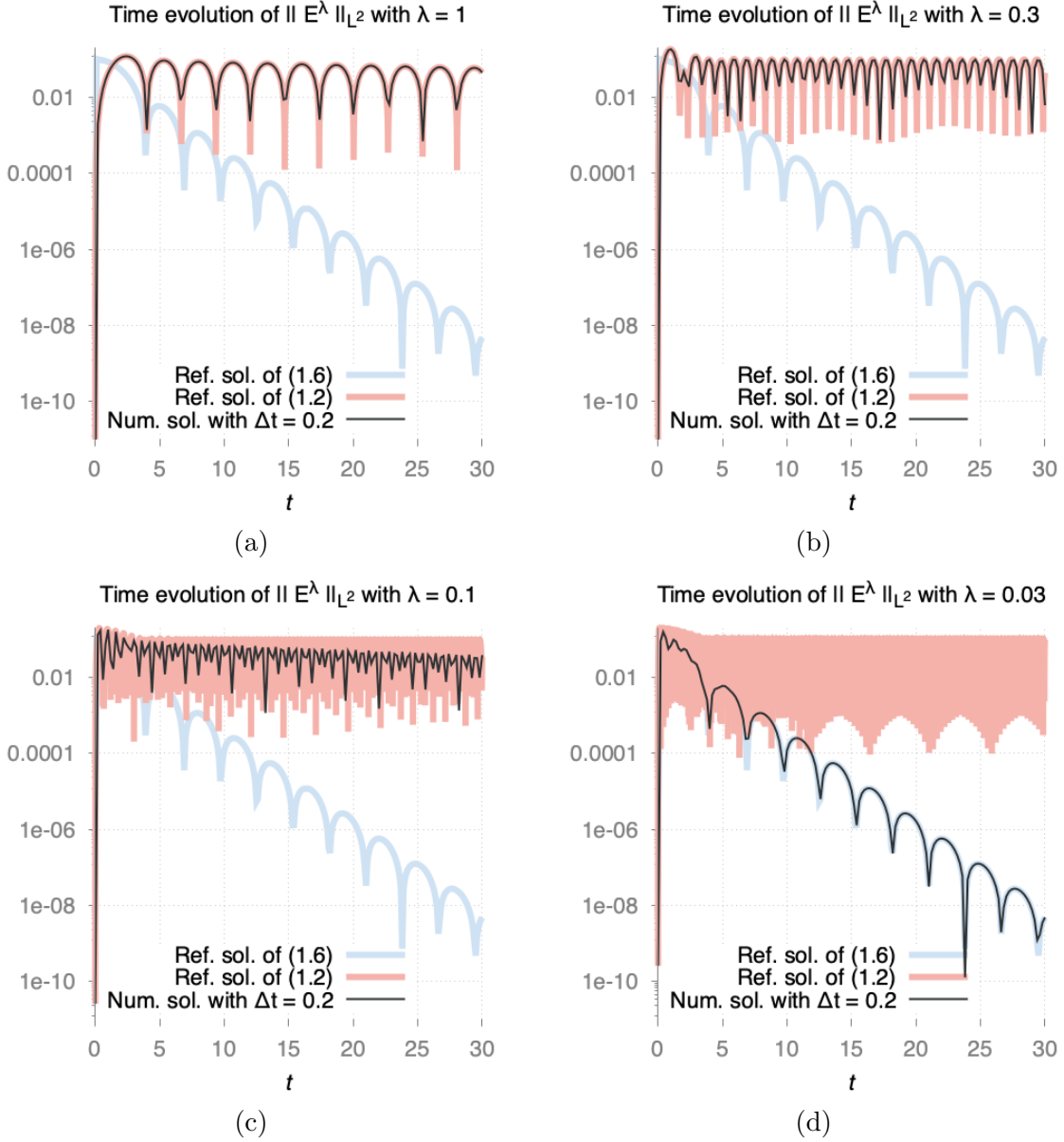


FIGURE 4.5. **Smooth perturbation of equilibrium test case:** time evolution of $\|E^\lambda\|_{L^2}$ in logarithmic scale with (a) $\lambda = 1$; (b) $\lambda = 3 \cdot 10^{-1}$; (c) $\lambda = 10^{-1}$ and (d) $\lambda = 3 \cdot 10^{-2}$.

As for the previous test case, we have $\rho_{\text{in}}(x) = 1$ and $j_{\text{in}}(x) = 0$, while high order moments are not spatially homogeneous. This configuration is such that the initial perturbation induces oscillations in the velocity space and, in this situation, one does not expect a fast convergence to zero of the slow component E_{slow}^λ . In fact, even in the quasineutral regime, velocity oscillations produce a sort of "echo" in the solution, so that the electric field exhibits slowly decaying oscillations with respect to time.

The reference solution is obtained using a fine mesh with $N_H = 1200$, $N_x = 500$, $\Delta t = 10^{-3}$ and the second order in time scheme presented in Section 3.4. This permits to capture both fast and slow scales phenomena for different values of the Debye length: $\lambda \in \{1, 10^{-1}, 10^{-2}, 10^{-3}\}$. In Figure 4.8 the time evolution of the L^2 norm of the electric field E^λ is shown while in Figure 4.9 we report the evolution of the slow component $E_{\text{slow}}^\lambda = \sqrt{2} \partial_x C_2^\lambda$. When $\lambda = 1$, the L^2 norm of the electric field is first damped and oscillates slowly, then, when $t \simeq 25$, the "echo" is observed. When $\lambda \ll 1$, the electric field E_{osc}^λ starts to oscillate with a frequency inversely proportional to λ , while the slow component $E_{\text{slow}}^\lambda = \sqrt{2} \partial_x C_2^\lambda$ is first strongly damped, then its amplitude increases again to reach a maximum around time $t \simeq 12.5$ and $t \simeq 25$ (see Figure 4.9). The fast oscillations of E_{slow}^λ have an amplitude of the order of $\delta \lambda^2$ (cf. Section 4.2) and they are not visible on Figure 4.9 since the amplitude of $\|\sqrt{2} \partial_x C_2^\lambda\|_{L^2}$ is above this threshold.

To investigate the asymptotic preserving property of the scheme we also performed numerical simulations using a coarse mesh, namely $N_x = 100$, $\Delta t = 0.1$ and $N_H = 1200$ for a wide variety of $\lambda \ll 1$. Notice that,

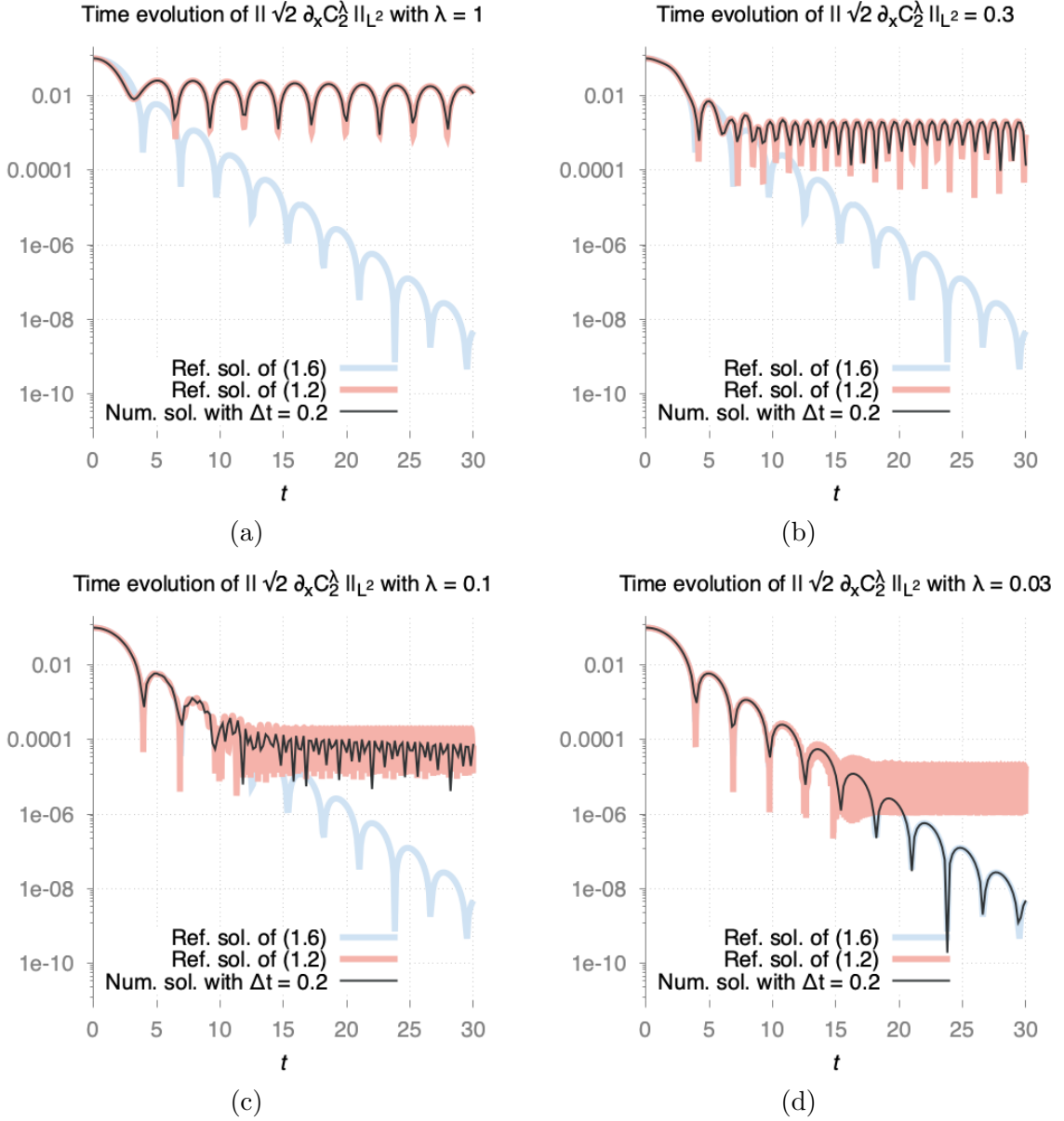


FIGURE 4.6. **Smooth perturbation of equilibrium test case:** time evolution of $\|\sqrt{2}\partial_x C_2^\lambda\|_{L^2}$ in logarithmic scale with (a) $\lambda = 1$; (b) $\lambda = 3 \cdot 10^{-1}$; (c) $\lambda = 10^{-1}$ and (d) $\lambda = 3.10^{-2}$.

in this case, a large number of Hermite modes is required to adequately describe oscillations in velocity. The numerical results are reported in Figures 4.8 and 4.9 and compared with the reference solution. For $\lambda = 1$ and 10^{-1} , the coarse mesh allows to describe precisely the time oscillations (Figures 4.8 and 4.9 (a)-(b)). When λ becomes smaller, the time step $\Delta t = 0.1$ is too large to provide an approximation of the fast scales, but the slow scale, corresponding to the quasineutral asymptotic model, is still well approximated (see Figures 4.8-(c) and (d) and 4.9-(c) and (d)). Finally, in Figure 4.10, we present several time snapshots of the perturbation $f^\lambda - \mathcal{M}$, where \mathcal{M} is the homogeneous Maxwellian equilibrium with $\lambda = 10^{-3}$. When $t = 25$, we observe the oscillation of f^λ around the equilibrium corresponding to the “echo” of the electric field previously discussed.

4.4. Two-stream instability. In this last example, we consider the two stream instability problem with initial distribution

$$(4.5) \quad f_{\text{in}}(x, v) = \frac{1}{6\sqrt{2\pi}T_{\text{in}}(x)} \left(1 + \frac{5|v|^2}{T_{\text{in}}(x)} \right) \exp\left(-\frac{|v|^2}{2T_{\text{in}}(x)}\right),$$

and with T_{in} given by

$$T_{\text{in}}(x) = 1 + \delta \cos(k_x x).$$

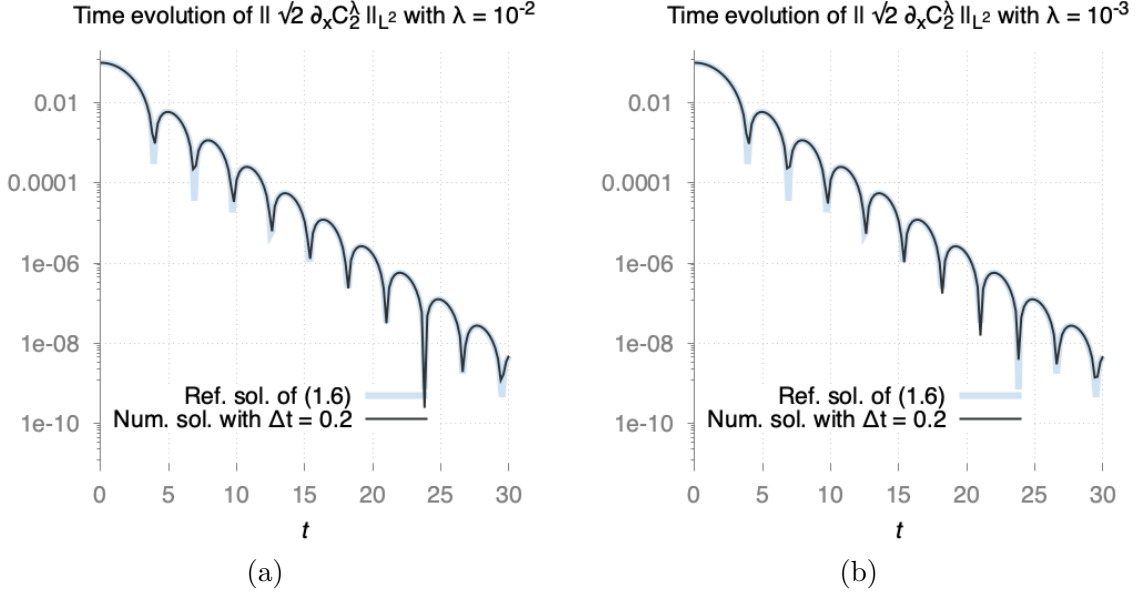


FIGURE 4.7. **Smooth perturbation of equilibrium test case:** time evolution of $\|\sqrt{2}\partial_x C_2^\lambda\|_{L^2}$ in logarithmic scale with (a) $\lambda = 10^{-2}$ and (b) $\lambda = 3 \cdot 10^{-3}$.

The other parameters are $\delta = 0.01$, $x \in [-6, 6]$ and $k_x = \pi/6$. For this initial data, the Vlasov-Poisson system (1.3) first develops an instability (called two-stream instability) which then stabilizes due to nonlinear effects. However, for the quasineutral limiting model, the situation is more intricate (see for instance [8] for the ill-posedness of the quasineutral model with the Landau collisional operator for a two-stream initial distribution or [25]). Thus, the quasineutral limit cannot be valid for all time intervals. It is important to notice that obtaining consistent numerical results for the Vlasov-Poisson system over long times is very difficult when λ is small, this is why we only took $\lambda = 0.04$ as the smallest values. However, even for these intermediate values, we get meaningful results, which help us to better understand the dynamics.

A reference solution is obtained with the second order scheme of Section 3.4 on a fine mesh with $N_H = 2000$, $N_x = 2000$ and $\Delta t = 10^{-4}$. This permits, as before, to observe both fast and slow scales of the solution for different values of λ . The time evolution of the L^2 norm of the electric field E^λ and of the slow component $E_{\text{slow}}^\lambda = \sqrt{2}\partial_x C_2^\lambda$ are again computed and shown in Figure 4.11 for different values of λ . We observe that the norm of E^λ on the time interval $[0, 6]$ strongly oscillates with a frequency inversely proportional to λ and grows exponentially with a rate independent of λ . For larger times, the instability rate increases as λ decreases. The evolution of E_{slow}^λ follows a similar growth dynamics, without exhibiting an oscillatory behavior. In the situation depicted, the rise of the instability is due to the slow part of the electric field, illustrating that the limiting system is not globally well-posed. Figure 4.12 presents the evolution of the same quantities as of Figure 4.11 with a scale of t/λ . This permits to understand that the instability is of the order of $O(e^{\kappa t/\lambda})$. These results show that when addressing the full scales, the numerical scheme allows for a better understanding of the instability phenomenon and the fact that the quasineutral limit is not valid on large time intervals for this initial data, which is consistent with the theoretical results of E. Grenier [25] and D. Han-Kwan and M. Hauray [27].

Finally, in Figure 4.13, we present the snapshots of the distribution function f^λ with $\lambda = 0.02$ at different time, when the instability occurs. At time $t = 8$, we observe several vortices in phase space (x, v) , which illustrates the complexity of the dynamics when λ is small.

5. CONCLUSION AND PERSPECTIVES

In this work, we proposed a new numerical scheme for the Vlasov-Poisson system able to overcome the strong restrictions due to the fast scale dynamics related to quasineutrality in plasmas. This discretization is quite different from those previously proposed in the literature, as it does not seek to reformulate the Poisson equation into an equivalent harmonic-type oscillator, but rather to discretize the Poisson equation simultaneously with the equations of the first moments. A significant difficulty in this study is that the quasineutral limit is not always valid for all initial conditions and all time intervals. On the one hand,

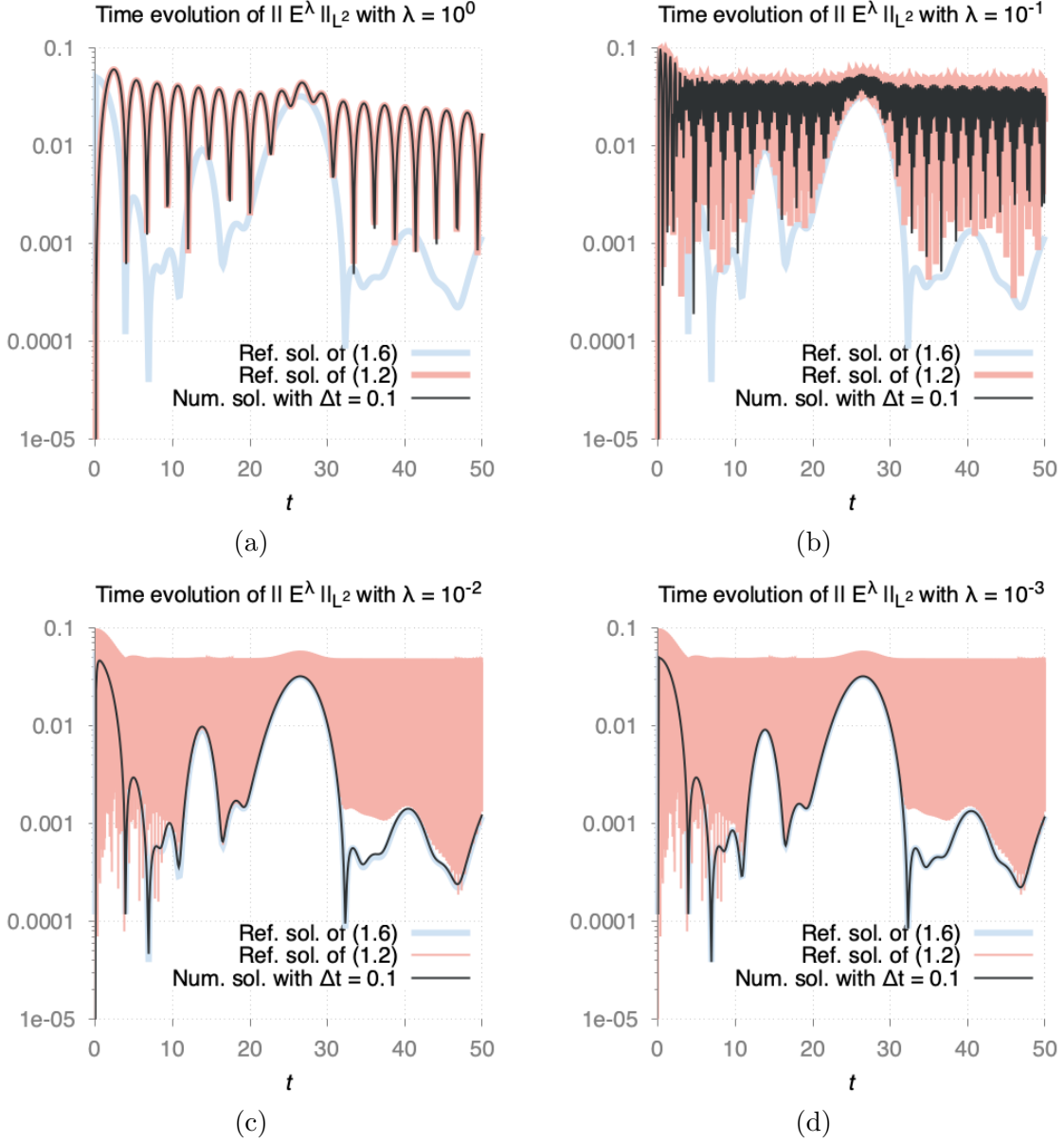


FIGURE 4.8. **Oscillatory perturbation from equilibrium test case:** time evolution of $\|E^\lambda\|_{L^2}$ in logarithmic scale with (a) $\lambda = 1$; (b) $\lambda = 10^{-1}$; (c) $\lambda = 10^{-2}$ and (d) $\lambda = 10^{-3}$.

our approach expands the distribution function in velocity space using Hermite functions, this enables to study the quasineutral limit by explicitly separating the oscillatory part from the rest of the solution and permits to obtain error estimates with respect to λ both at the continuous and the discrete levels. On the other hand, we propose a time-splitting method, where the first step involves solving the linearized system around the Maxwellian stationary state and the second step solves the nonlinear remaining part of the system.

In a second part, we have performed several numerical simulations for stable and unstable initial conditions. We have recovered the theoretical convergence order estimates for well-prepared initial data. In these situations and when the time step is very large compared to λ , the numerical scheme filters out the rapid oscillations and captures the asymptotic limit. Moreover, our numerical simulations indicate that when the quasineutral limit is not valid on large time intervals, the scheme is not stable for all λ and the numerical solution may be unstable. Understanding the quasineutral limit remains an open problem within the framework of kinetic theory, our numerical results are consistent with those available in the mathematical analysis literature [25, 27, 8] and we expect to provide novel insights that could guide the demonstration of the required mathematical results.

Concerning the analysis of the numerical scheme, it appears crucial to gain a better understanding of the stability of the scheme with respect to the discretization parameters and the Debye length. Furthermore,

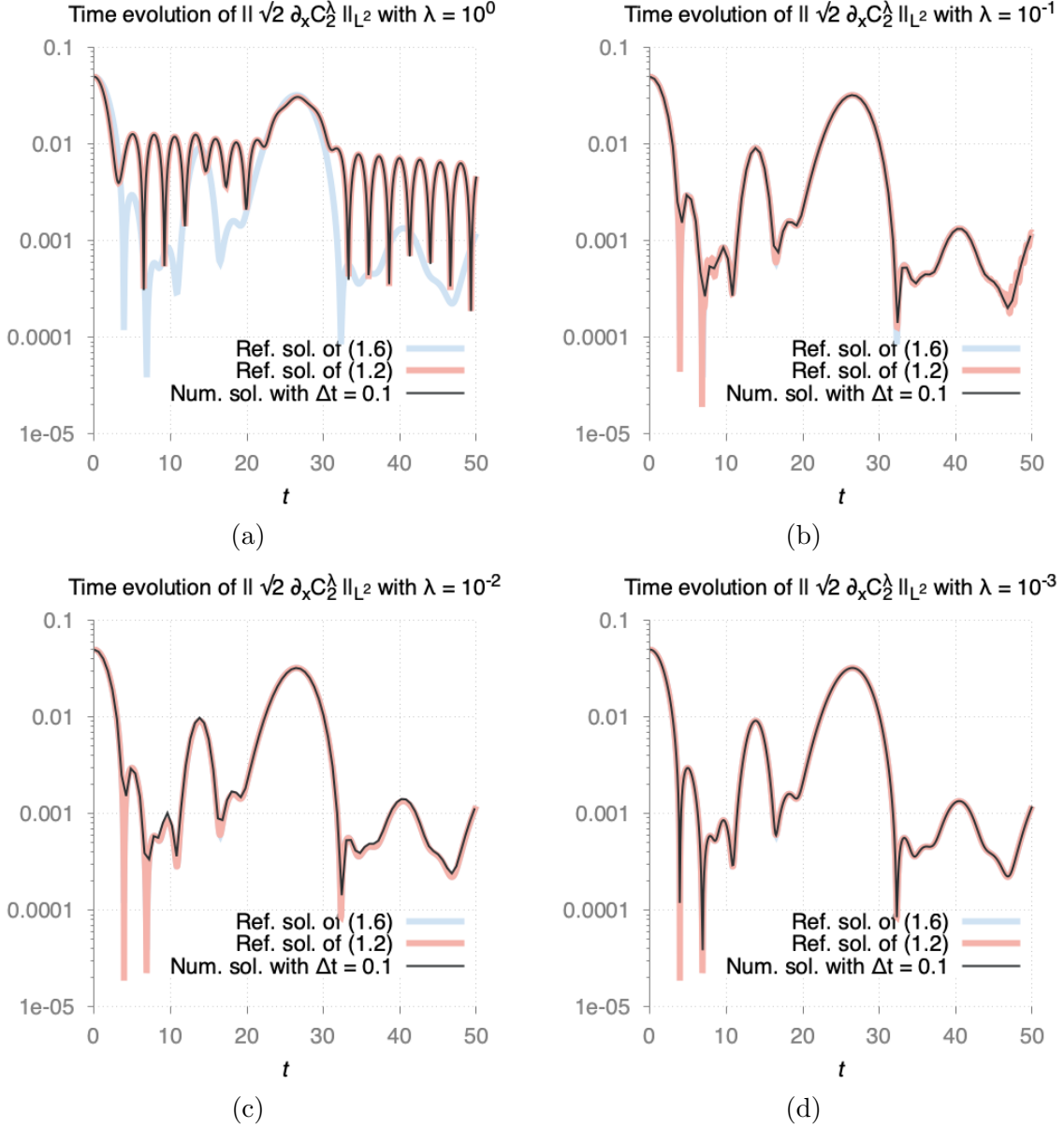


FIGURE 4.9. **Oscillatory perturbation from equilibrium test case:** time evolution of $\|\sqrt{2}\partial_x C_2^\lambda\|_{L^2}$ in logarithmic value with (a) $\lambda = 1$; (b) $\lambda = 10^{-1}$; (c) $\lambda = 10^{-2}$ and (d) $\lambda = 10^{-3}$.

extending the proposed method to the multi-dimensional case [4] represents an important step for realistic applications.

ACKNOWLEDGEMENT

Francis Filbet and Marie-Hélène Vignal are partially funded by the ANR Project Muffin (ANR-19-CE46-0004). Alain Blaustein acknowledges the support of the CDP C2EMPI, as well as the French State under the France-2030 programme, the University of Lille, the Initiative of Excellence of the University of Lille, the European Metropolis of Lille for their funding and support of the R-CDP-24-004-C2EMPI project.

APPENDIX A. PROOF OF PROPOSITION 2.1

We fix some time $t \in [0, T]$ and prove that the right hand side in the Duhamel formula (2.10) is of order $\lambda^{1-\alpha}$. To this aim, we distinguish linear and nonlinear terms in \mathbf{S}^λ . Then, to identify the nonlinear terms and their scaling in λ , we replace $\partial_t C_2^\lambda$ according to (2.5) with $k = 2$ and C_0^λ according to the second line of (2.5) in \mathbf{S}^λ , we obtain

$$(A.1) \quad \mathbf{U}^\lambda(t) = - \int_0^t \exp\left(\frac{s-t}{\lambda} J\right) (\mathbf{N}^\lambda + \mathbf{L}^\lambda)(s) ds,$$

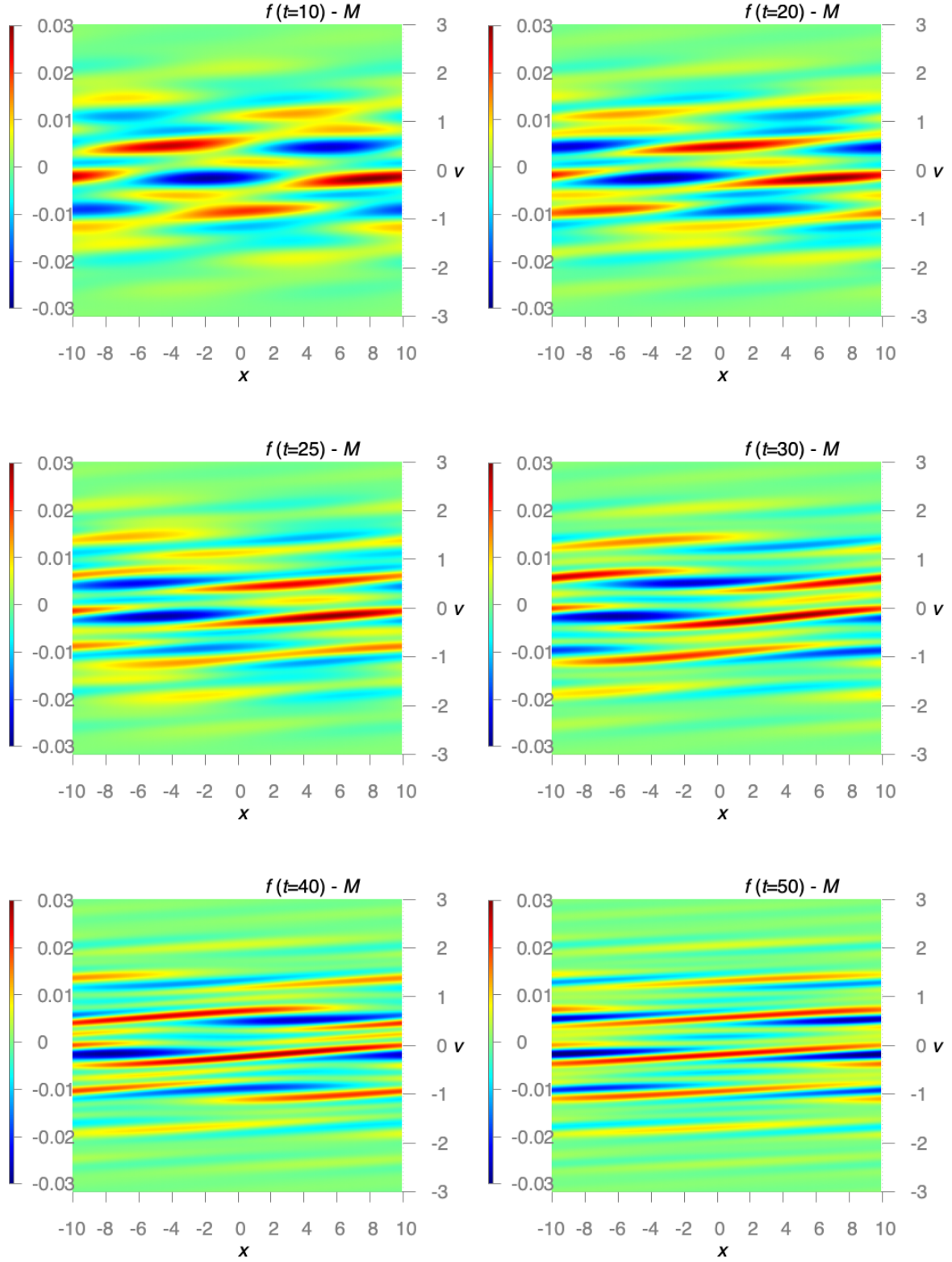


FIGURE 4.10. **Oscillatory perturbation from equilibrium test case:** snapshots of the distribution function $f^\lambda - \mathcal{M}$ at time $t = 10 ; 20 ; 25 ; 30 ; 40$ and 50 for $\lambda = 10^{-3}$.

where \mathbf{N}^λ and \mathbf{L}^λ are given as follows

$$\mathbf{N}^\lambda = 2T_0^{1/2}\partial_x \begin{pmatrix} C_1^\lambda E^\lambda \\ 0 \end{pmatrix} - \frac{\lambda}{2}\partial_x \begin{pmatrix} 0 \\ |E^\lambda|^2 \end{pmatrix}; \quad \mathbf{L}^\lambda = -T_0^{3/2}\partial_x^2 \begin{pmatrix} \sqrt{6}C_3^\lambda + 2C_1^\lambda \\ 0 \end{pmatrix} + \lambda T_0\partial_x^2 \begin{pmatrix} 0 \\ E^\lambda \end{pmatrix}.$$

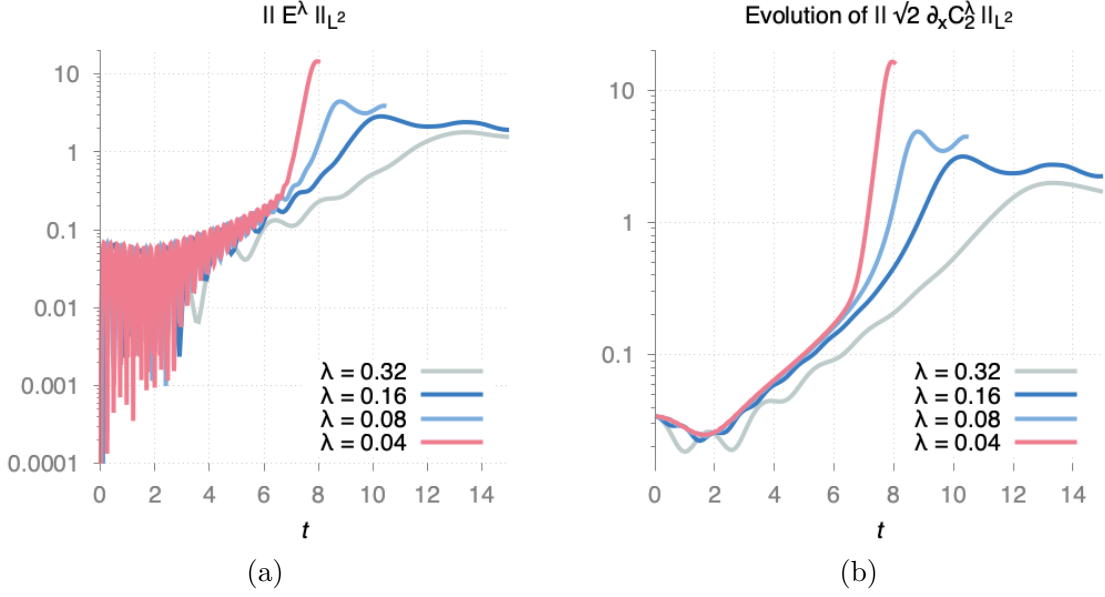


FIGURE 4.11. **Two-stream instability test case:** time evolution of (a) $\|E^\lambda\|_{L^2}$ and (b) $\|\sqrt{2}\partial_x C_2^\lambda\|_{L^2}$ in logarithmic scale.

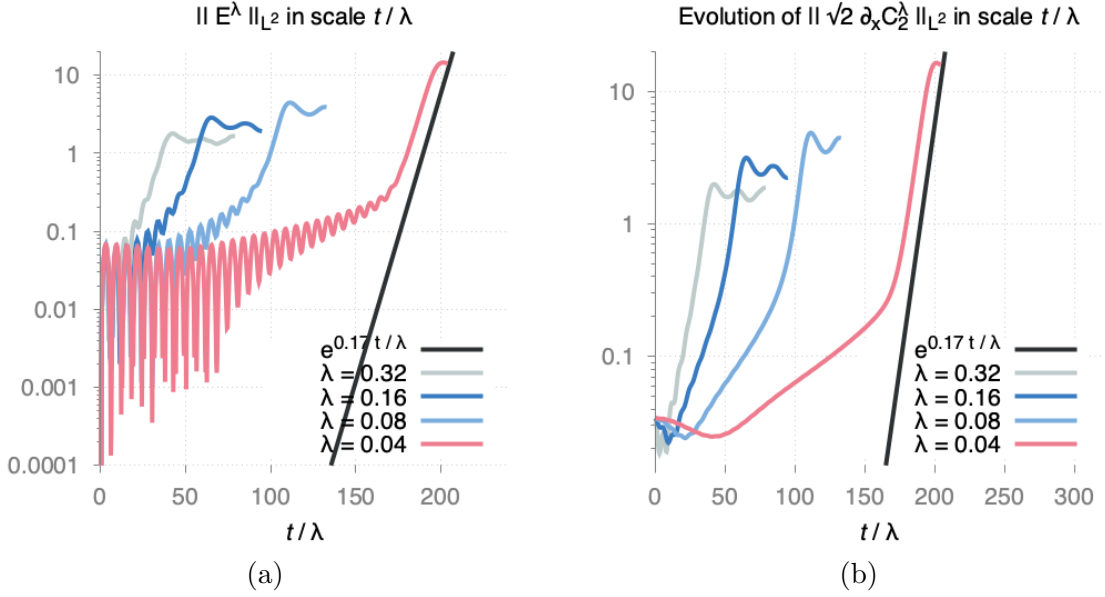


FIGURE 4.12. **Two-stream instability test case:** evolution of (a) $\|E^\lambda\|_{L^2}$ and (b) $\|\sqrt{2}\partial_x C_2^\lambda\|_{L^2}$ in logarithmic scale with respect to t/λ .

To control the contribution of \mathbf{L}^λ , we apply a standard Laplace method for oscillating integrals and use assumptions (2.11)-(2.12) to control the time derivatives of C_1^λ and C_3^λ . The nonlinear contribution \mathbf{N}^λ is more intricate since $|E^\lambda|^2$ may behave like $O(\lambda^{-2\alpha})$. However, we show that the singular terms are solely due to fast oscillations, which are small as $\lambda \rightarrow 0$.

First, we replace C_1^λ in \mathbf{N}^λ according to the Ampère equation (2.7), which yields

$$\mathbf{N}^\lambda(s) = -\lambda^2 \partial_s \partial_x \begin{pmatrix} |E^\lambda(s)|^2 \\ 0 \end{pmatrix} - \frac{\lambda}{2} \partial_x \begin{pmatrix} 0 \\ |E^\lambda(s)|^2 \end{pmatrix},$$

where we also applied the relation $2E^\lambda \partial_s E^\lambda = \partial_s |E^\lambda|^2$. Multiplying the latter formula by $\exp(sJ/\lambda)$, applying Leibniz rule for products and using the definition of J below (1.11), yields

$$(A.2) \quad \exp\left(\frac{s}{\lambda}J\right) \cdot \mathbf{N}^\lambda(s) = -\lambda^2 \partial_s \left(\exp\left(\frac{s}{\lambda}J\right) \cdot \partial_x \begin{pmatrix} |E^\lambda(s)|^2 \\ 0 \end{pmatrix} \right) - \frac{3\lambda}{2} \exp\left(\frac{s}{\lambda}J\right) \cdot \partial_x \begin{pmatrix} 0 \\ |E^\lambda(s)|^2 \end{pmatrix}.$$

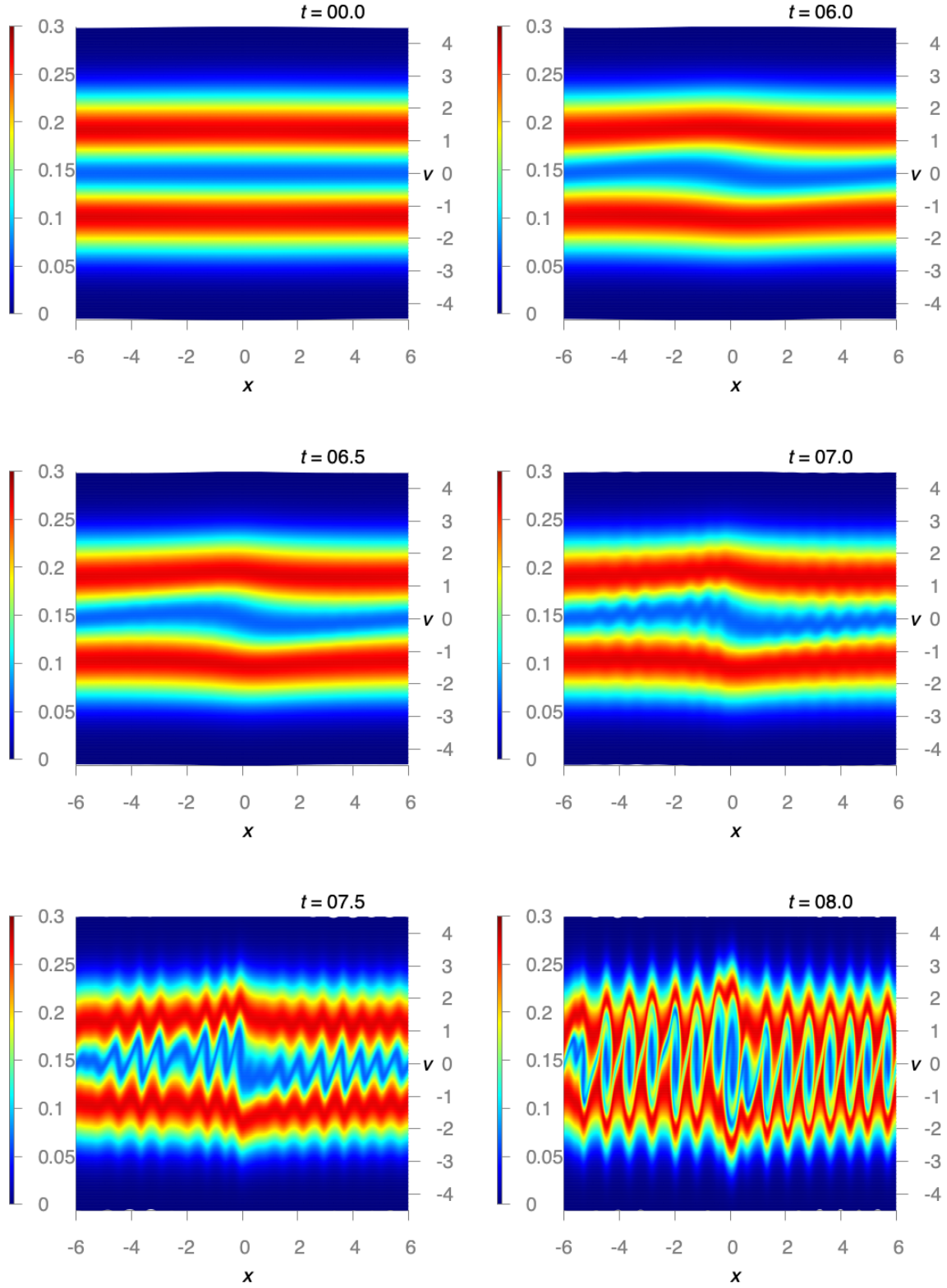


FIGURE 4.13. **Two-stream instability test case:** snapshots of the distribution function f^λ at time $t = 0 ; 6 ; 6.5 ; 7 ; 7.5$ and 8 for $\lambda = 0.04$.

The main difficulty comes from the second term in the latter right hand side. Hence, we estimate it by computing explicitly the contribution of the singular terms in the expansion of E^λ as $\lambda \rightarrow 0$. More precisely, we substitute E^λ thanks to the relation

$$E^\lambda = \mathbf{U}_1^\lambda + E_{\text{slow}}^\lambda + E_{\text{osc}}^\lambda,$$

where \mathbf{U}_1^λ denotes the first component of \mathbf{U}^λ and where E_{osc}^λ , given by (2.14), contains the singular terms in the expansion of E^λ . Hence, we have

$$\frac{1}{2} \partial_x |E^\lambda|^2 = \mathbf{U}_1^\lambda \partial_x E^\lambda + E_{\text{osc}}^\lambda \partial_x \mathbf{U}_1^\lambda + \frac{1}{2} \partial_x |E_{\text{osc}}^\lambda|^2 + E_{\text{osc}}^\lambda \partial_x E_{\text{slow}}^\lambda + E_{\text{slow}}^\lambda \partial_x E^\lambda,$$

We replace $|E^\lambda|^2$ according to the latter relation in the second term on the right hand side of (A.2) and obtain

$$(A.3) \quad \exp\left(\frac{s}{\lambda} J\right) \cdot \mathbf{N}^\lambda = -\lambda^2 \partial_s \left(\exp\left(\frac{s}{\lambda} J\right) \cdot \mathbf{N}_1^\lambda \right) - \exp\left(\frac{s}{\lambda} J\right) \cdot \left(A_1 \mathbf{U}_1^\lambda + A_2 \partial_x \mathbf{U}_1^\lambda + \lambda \mathbf{N}_2^\lambda \right),$$

where $(\mathbf{N}_1^\lambda, \mathbf{N}_2^\lambda)$ and (A_1, A_2) are given as follows

$$\mathbf{N}_1^\lambda(s) = \partial_x \begin{pmatrix} |E^\lambda(s)|^2 \\ 0 \end{pmatrix}; \quad A_1(s) = 3\lambda \begin{pmatrix} 0 \\ \partial_x E^\lambda(s) \end{pmatrix}; \quad A_2(s) = 3\lambda \begin{pmatrix} 0 \\ E_{\text{osc}}^\lambda(s) \end{pmatrix};$$

whereas

$$\mathbf{N}_2^\lambda(s) = 3 \begin{pmatrix} 0 \\ \frac{1}{2} \partial_x |E_{\text{osc}}^\lambda(s)|^2 + E_{\text{osc}}^\lambda(s) \partial_x E_{\text{slow}}^\lambda(s) + E_{\text{slow}}^\lambda(s) \partial_x E^\lambda(s) \end{pmatrix} (s).$$

Then, we substitute \mathbf{N}^λ in (A.1) according to (A.3) and obtain

$$(A.4) \quad \mathbf{U}^\lambda(t) = \int_0^t \exp\left(\frac{s-t}{\lambda} J\right) \cdot \left(A_1(s) \mathbf{U}_1^\lambda(s) + A_2(s) \partial_x \mathbf{U}_1^\lambda(s) \right) ds + B(t),$$

where A_1 and A_2 are given below (A.3) and B gathers all the other terms, that is,

$$B(t) = \int_0^t \exp\left(\frac{s-t}{\lambda} J\right) \cdot (\lambda \mathbf{N}_2^\lambda(s) - \mathbf{L}^\lambda(s)) ds + \lambda^2 \mathbf{N}_1^\lambda(t) - \lambda^2 \exp\left(-\frac{t}{\lambda} J\right) \cdot \mathbf{N}_1^\lambda(0),$$

where \mathbf{L}^λ is given in (A.1) whereas $\mathbf{N}_1^\lambda, \mathbf{N}_2^\lambda$ are given in (A.3).

Our strategy is to prove that A_1, A_2 and B are of order $O(\lambda^{1-\alpha})$ and iterate the Duhamel formula (A.4) to gain powers of λ .

Step 1. Upper bound of A_1, A_2 and B . Let us estimate A_1, A_2 and B , given in (A.4), starting with B , which contains the main difficulty, due to the contribution of \mathbf{N}_2^λ . To estimate B , we reformulate the first term of \mathbf{L}^λ , defined in (A.1), which is given by

$$\mathbf{L}_1^\lambda = -T_0^{3/2} \partial_x^2 \begin{pmatrix} \sqrt{6} C_3^\lambda + 2 C_1^\lambda \\ 0 \end{pmatrix}.$$

We multiply \mathbf{L}_1^λ by $\exp(sJ/\lambda)$ and apply Leibniz rule for products, which yields

$$\exp\left(\frac{s}{\lambda} J\right) \cdot \mathbf{L}_1^\lambda = \lambda J^{-1} \partial_s \left(\exp\left(\frac{s}{\lambda} J\right) \cdot \mathbf{L}_1^\lambda \right) - \lambda J^{-1} \exp\left(\frac{s}{\lambda} J\right) \cdot \partial_t \mathbf{L}_1^\lambda.$$

Next, since $J^{-1} = -J$ and since J and $\exp(\frac{s}{\lambda} J)$ commute, we obtain

$$\exp\left(\frac{s}{\lambda} J\right) \cdot \mathbf{L}_1^\lambda = -\lambda \partial_s \left(\exp\left(\frac{s}{\lambda} J\right) \cdot T_0^{3/2} \partial_x^2 \begin{pmatrix} 0 \\ \sqrt{6} C_3^\lambda + 2 C_1^\lambda \end{pmatrix} \right) + \lambda \exp\left(\frac{s}{\lambda} J\right) \cdot T_0^{3/2} \partial_t \partial_x^2 \begin{pmatrix} 0 \\ \sqrt{6} C_3^\lambda + 2 C_1^\lambda \end{pmatrix}.$$

According to the latter relation, the product between $\exp(sJ/\lambda)$ and \mathbf{L}^λ satisfies

$$(A.5) \quad \exp\left(\frac{s}{\lambda} J\right) \cdot \mathbf{L}^\lambda = -\lambda \partial_s \left(\exp\left(\frac{s}{\lambda} J\right) \cdot \mathbf{L}_2^\lambda \right) + \lambda \exp\left(\frac{s}{\lambda} J\right) \cdot \mathbf{L}_3^\lambda,$$

where \mathbf{L}_2^λ and \mathbf{L}_3^λ are given as follows

$$\mathbf{L}_2^\lambda = T_0^{3/2} \partial_x^2 \begin{pmatrix} 0 \\ \sqrt{6} C_3^\lambda + 2 C_1^\lambda \end{pmatrix}; \quad \mathbf{L}_3^\lambda = T_0^{3/2} \partial_s \partial_x^2 \begin{pmatrix} 0 \\ \sqrt{6} C_3^\lambda + 2 C_1^\lambda \end{pmatrix} + T_0 \begin{pmatrix} 0 \\ \partial_x^2 E^\lambda \end{pmatrix}.$$

We replace \mathbf{L}^λ according to (A.5) in the definition of B in (A.4), we find

$$B(t) = \lambda \int_0^t \exp\left(\frac{s-t}{\lambda} J\right) \cdot (\mathbf{N}_2^\lambda - \mathbf{L}_3^\lambda)(s) ds + \lambda (\lambda \mathbf{N}_1^\lambda + \mathbf{L}_2^\lambda)(t) - \lambda \exp\left(-\frac{t}{\lambda} J\right) \cdot (\lambda \mathbf{N}_1^\lambda + \mathbf{L}_2^\lambda)(0).$$

We take the L^2 norm of the l -th derivative and apply the triangle inequality in the latter relation

$$(A.6) \quad \begin{aligned} \left\| \partial_x^l B(t) \right\|_{L^2} &\leq \lambda \left\| \partial_x^l \int_0^t \exp\left(\frac{s}{\lambda} J\right) \cdot \mathbf{N}_2^\lambda(s) ds \right\|_{L^2} + \lambda \left\| \partial_x^l \int_0^t \exp\left(\frac{s}{\lambda} J\right) \cdot \mathbf{L}_3^\lambda(s) ds \right\|_{L^2} \\ &\quad + \lambda^2 \left\| \partial_x^l \mathbf{N}_1^\lambda(t) \right\|_{L^2} + \lambda \left\| \partial_x^l \mathbf{L}_2^\lambda(t) \right\|_{L^2} + \lambda^2 \left\| \partial_x^l \mathbf{N}_1^\lambda(0) \right\|_{L^2} + \lambda \left\| \partial_x^l \mathbf{L}_2^\lambda(0) \right\|_{L^2}. \end{aligned}$$

To estimate the first term in the right hand side of (A.6), we substitute \mathbf{N}_2^λ according to its definition below (A.3) and apply the triangle inequality, which yields

$$\lambda \left\| \partial_x^l \int_0^t \exp\left(\frac{s}{\lambda} J\right) \cdot \mathbf{N}_2^\lambda ds \right\|_{L^2} \leq \mathcal{N}_{21}(t) + \mathcal{N}_{22}(t),$$

where

$$\begin{cases} \mathcal{N}_{21}(t) = \frac{3\lambda}{2} \left\| \partial_x^l \int_0^t \exp\left(\frac{s}{\lambda} J\right) \cdot \partial_x \begin{pmatrix} 0 \\ |E_{\text{osc}}^\lambda|^2 \end{pmatrix} ds \right\|_{L^2}, \\ \mathcal{N}_{22}(t) = 3\lambda \left\| \partial_x^l \int_0^t \exp\left(\frac{s}{\lambda} J\right) \cdot \begin{pmatrix} 0 \\ E_{\text{osc}}^\lambda \sqrt{2} T_0 \partial_x^2 C_2^\lambda + \sqrt{2} T_0 \partial_x C_2^\lambda \partial_x E^\lambda \end{pmatrix} ds \right\|_{L^2}. \end{cases}$$

The estimate for $\mathcal{N}_{21}(t)$ is the most intricate since E_{osc}^λ , given by (2.14), is of order $O(\lambda^{-\alpha})$. We compute the time integral in $\mathcal{N}_{21}(t)$ explicitly and show that the singularity cancels due to the fast oscillations of E_{osc}^λ . To make these computations more tractable, we identify $\exp(sJ/\lambda)$ and E_{osc}^λ in $\mathcal{N}_{21}(t)$ with their complex representation

$$\exp\left(\frac{s}{\lambda} J\right) = e^{-i\frac{s}{\lambda}} \quad ; \quad \begin{pmatrix} 0 \\ |E_{\text{osc}}^\lambda|^2 \end{pmatrix} = i |E_{\text{osc}}^\lambda|^2 \quad ; \quad E_{\text{osc}}^\lambda(s) = \frac{ze^{i\frac{s}{\lambda}} + \bar{z}e^{-i\frac{s}{\lambda}}}{2},$$

where the time independent complex number z is given by

$$(A.7) \quad z = \left(E^\lambda - \sqrt{2} T_0 \partial_x C_2^\lambda \right)(0) + \frac{i\sqrt{T_0}}{\lambda} C_1^\lambda(0).$$

We reformulate $\mathcal{N}_{21}(t)$ according to the latter relations

$$\mathcal{N}_{21}(t) = \frac{3\lambda}{2} \left\| \partial_x^{l+1} \int_0^t e^{-i\frac{s}{\lambda}} i \left| \frac{ze^{i\frac{s}{\lambda}} + \bar{z}e^{-i\frac{s}{\lambda}}}{2} \right|^2 ds \right\|_{L^2}$$

and expand the square in the latter expression and compute the time integral explicitly:

$$\mathcal{N}_{21}(t) = \frac{3\lambda^2}{2} \left\| \partial_x^{l+1} \left(\frac{|z|^2}{2} \left(1 - e^{-i\frac{t}{\lambda}} \right) + \frac{z^2}{4} \left(e^{i\frac{t}{\lambda}} - 1 \right) + \frac{\bar{z}^2}{12} \left(1 - e^{-3i\frac{t}{\lambda}} \right) \right) \right\|_{L^2}.$$

Then, we apply Leibniz rule to develop the derivatives in x of order $l+1$ and estimate each product thanks to Cauchy-Schwarz inequality, which yields

$$\mathcal{N}_{21}(t) \leq C \lambda^2 \|z\|_{W^{l+1,4}}^2,$$

for some constant C depending on $l \geq 0$. We replace z according to its definition (A.7) and apply the triangle inequality in the latter relation and obtain

$$\mathcal{N}_{21}(t) \leq C \left(\lambda^2 \left\| C_2^\lambda(0) \right\|_{W^{l+2,4}}^2 + \lambda^2 \left\| E^\lambda(0) \right\|_{W^{l+1,4}}^2 + \left\| C_1^\lambda(0) \right\|_{W^{l+1,4}}^2 \right).$$

To estimate $\mathcal{N}_{22}(t)$, we bound the time integral thanks to Jensen inequality and then take the supremum in time, this yields

$$\mathcal{N}_{22}(t) \leq 3\lambda t \sup_{0 \leq s \leq T} \left(\left\| \partial_x^l \left(E_{\text{osc}}^\lambda(s) \sqrt{2} T_0 \partial_x^2 C_2^\lambda(s) \right) \right\|_{L^2} + \left\| \partial_x^l \left(\sqrt{2} T_0 \partial_x C_2^\lambda(s) \partial_x E^\lambda(s) \right) \right\|_{L^2} \right).$$

Then, we apply Leibniz rule to develop the derivatives of order l and estimate each product thanks to Cauchy-Schwarz inequality, which yields

$$\mathcal{N}_{22}(t) \leq C \lambda \sup_{0 \leq s \leq T} \left(\left\| C_2^\lambda(s) \right\|_{W^{l+2,4}} \left\| E_{\text{osc}}^\lambda(s) \right\|_{W^{l,4}} + \left\| C_2^\lambda(s) \right\|_{W^{l+1,4}} \left\| E^\lambda(s) \right\|_{W^{l+1,4}} \right),$$

for some constant C depending on $l \geq 0$, on the final time T and the temperature T_0 . We estimate E_{osc}^λ with the triangular inequality, which yields

$$\mathcal{N}_{22}(t) \leq C \lambda \sup_{0 \leq s \leq T} \left(\|C_2^\lambda(s)\|_{W^{l+2,4}} (\|E^\lambda(0)\|_{W^{l,4}} + \|C_2^\lambda(0)\|_{W^{l+1,4}} + \lambda^{-1} \|C_1^\lambda(0)\|_{W^{l,4}} + \|E^\lambda(s)\|_{W^{l+1,4}}) \right),$$

and then apply Young inequality to estimate each product, which yields

$$\mathcal{N}_{22}(t) \leq C \sup_{0 \leq s \leq T} \left(\lambda^{1-\alpha} \|C_2^\lambda(s)\|_{W^{l+2,4}}^2 + \lambda^{\alpha-1} \|C_1^\lambda(0)\|_{W^{l,4}}^2 + \lambda^{1+\alpha} \|E^\lambda(s)\|_{W^{l+1,4}}^2 \right),$$

for all $0 < \lambda < 1$. Gathering our estimates on \mathcal{N}_{21} and \mathcal{N}_{22} , we obtain

$$(A.8) \quad \lambda \left\| \partial_x^l \int_0^t \exp\left(\frac{s}{\lambda} J\right) \cdot \mathbf{N}_2^\lambda ds \right\|_{L^2} \leq C \left(\lambda^{\alpha-1} \|C_1^\lambda(0)\|_{W^{l+1,4}}^2 + \lambda^{1+\alpha} \sup_{0 \leq s \leq T} \|E^\lambda(s)\|_{W^{l+1,4}}^2 \right) \\ + C \lambda^{1-\alpha} \sup_{0 \leq s \leq T} \|C_2^\lambda(s)\|_{W^{l+2,4}}^2,$$

for all $0 < \lambda < 1$ and for some constant C depending on $l \geq 0$, on the final time T and the temperature T_0 . We now estimate the second term in the right hand side (A.6) thanks to Jensen inequality

$$\lambda \left\| \partial_x^l \int_0^t \exp\left(\frac{s}{\lambda} J\right) \cdot \mathbf{L}_3^\lambda ds \right\|_{L^2} \leq \lambda t \sup_{0 \leq s \leq T} \left\| \partial_x^l \mathbf{L}_3^\lambda(s) \right\|_{L^2},$$

where \mathbf{L}_3^λ is defined below (A.5). Then, we substitute the time derivatives of C_1^λ and C_3^λ in the expression of \mathbf{L}_3^λ thanks to the first line of (2.5) with $k = 1$ and $k = 3$ respectively, which yields

$$\lambda \left\| \partial_x^l \int_0^t \exp\left(\frac{s}{\lambda} J\right) \cdot \mathbf{L}_3^\lambda ds \right\|_{L^2} \leq \\ \lambda T_0 t \sup_{0 \leq s \leq T} \left\| \partial_x^{l+2} \left(\sqrt{18} E^\lambda C_2^\lambda - \sqrt{18} T_0 \partial_x C_2^\lambda - \sqrt{24} T_0 \partial_x C_4^\lambda + 2 E^\lambda C_0^\lambda - 2 T_0 \partial_x C_0^\lambda - 2 \sqrt{2} T_0 \partial_x C_2^\lambda + E^\lambda \right) \right\|_{L^2}.$$

We apply the triangle inequality and obtain

$$\lambda \left\| \partial_x^l \int_0^t \exp\left(\frac{s}{\lambda} J\right) \cdot \mathbf{L}_3^\lambda ds \right\|_{L^2} \leq C \lambda \sup_{0 \leq s \leq T} \left(\left\| \partial_x^{l+2} E^\lambda(s) \right\|_{L^2} + \left\| \partial_x^{l+2} (E^\lambda C_2^\lambda)(s) \right\|_{L^2} + \left\| \partial_x^{l+2} (E^\lambda C_0^\lambda)(s) \right\|_{L^2} \right) \\ + C \lambda \sup_{0 \leq s \leq T} \left(\left\| \partial_x^{l+3} C_2^\lambda(s) \right\|_{L^2} + \left\| \partial_x^{l+3} C_4^\lambda(s) \right\|_{L^2} + \left\| \partial_x^{l+3} C_0^\lambda(s) \right\|_{L^2} \right),$$

for some constant C depending on the final time T and the temperature T_0 . Then, we apply Leibniz rule to develop the nonlinear terms and estimate each product thanks to Young inequality

$$(A.9) \quad \lambda \left\| \partial_x^l \int_0^t \exp\left(\frac{s}{\lambda} J\right) \cdot \mathbf{L}_3^\lambda ds \right\|_{L^2} \leq C \sup_{0 \leq s \leq T} \left(\lambda \left\| \partial_x^{l+2} E^\lambda(s) \right\|_{L^2}, \lambda^{1+\alpha} \|E^\lambda(s)\|_{W^{l+2,4}}^2 \right) \\ + C \sup_{\substack{0 \leq s \leq T \\ k=0,2,4}} \left(\lambda \left\| \partial_x^{l+3} C_k^\lambda(s) \right\|_{L^2}, \lambda^{1-\alpha} \|C_k^\lambda(s)\|_{W^{l+2,4}}^2 \right),$$

for some constant C depending on $l \geq 0$, on the final time T and the temperature T_0 . We use the same method to estimate the last four terms on the right hand side of (A.6) and obtain

$$(A.10) \quad \lambda^2 \left\| \partial_x^l \mathbf{N}_1^\lambda(t) \right\|_{L^2} + \lambda \left\| \partial_x^l \mathbf{L}_2^\lambda(t) \right\|_{L^2} + \lambda^2 \left\| \partial_x^l \mathbf{N}_1^\lambda(0) \right\|_{L^2} + \lambda \left\| \partial_x^l \mathbf{L}_2^\lambda(0) \right\|_{L^2} \\ \leq C \lambda^2 \sup_{0 \leq s \leq T} \left(\|E^\lambda(s)\|_{W^{l+1,4}}^2 \right) + C \lambda \sup_{\substack{0 \leq s \leq T \\ k=1,3}} \left(\left\| \partial_x^{l+2} C_k^\lambda(s) \right\|_{L^2} \right),$$

for some constant C depending on $l \geq 0$ and on the temperature T_0 . Gathering estimates (A.8), (A.9) and (A.10) in (A.6), we find

$$\left\| \partial_x^l B(t) \right\|_{L^2} \leq C \left(\lambda^{\alpha-1} \|C_1^\lambda(0)\|_{W^{l+1,4}}^2 + \sup_{0 \leq s \leq T} \left(\lambda \left\| \partial_x^{l+2} E^\lambda(s) \right\|_{L^2}, \lambda^{1+\alpha} \|E^\lambda(s)\|_{W^{l+2,4}}^2 \right) \right) \\ + C \sup_{\substack{0 \leq s \leq T \\ 0 \leq k \leq 4}} \left(\lambda \|C_k^\lambda(s)\|_{H^{l+3}}, \lambda^{1-\alpha} \|C_k^\lambda(s)\|_{W^{l+2,4}}^2 \right),$$

for all $0 < \lambda < 1$ and for some constant C depending on $l \geq 0$, on the final time T and the temperature T_0 . We sum the latter estimate over all $l \leq n$ and take the supremum in t on the left hand side, which yields

$$\begin{aligned} \sup_{0 \leq t \leq T} \|B(t)\|_{H^n} &\leq C \left(\lambda^{\alpha-1} \|C_1^\lambda(0)\|_{W^{n+1,4}}^2 + \sup_{0 \leq t \leq T} \left(\lambda \|E^\lambda(t)\|_{H^{n+2}}, \lambda^{1+\alpha} \|E^\lambda(t)\|_{W^{n+2,4}}^2 \right) \right) \\ &\quad + C \sup_{\substack{0 \leq t \leq T \\ 0 \leq k \leq 4}} \left(\lambda \|C_k^\lambda(t)\|_{H^{n+3}}, \lambda^{1-\alpha} \|C_k^\lambda(t)\|_{W^{n+2,4}}^2 \right), \end{aligned}$$

for all $0 < \lambda < 1$ and $n \geq 0$, where the constant C depends on $n \geq 0$, on the final time T and the temperature T_0 . We bound $L^2(\mathbb{T})$ norms with their $L^4(\mathbb{T})$ counterparts, which yields

$$\begin{aligned} \sup_{0 \leq t \leq T} \|B(t)\|_{H^n} &\leq C \left(\lambda^{\alpha-1} \|C_1^\lambda(0)\|_{W^{n+1,4}}^2 + \sup_{0 \leq t \leq T} \left(\lambda \|E^\lambda(t)\|_{W^{n+2,4}}, \lambda^{1+\alpha} \|E^\lambda(t)\|_{W^{n+2,4}}^2 \right) \right) \\ &\quad + C \sup_{\substack{0 \leq t \leq T \\ 0 \leq k \leq 4}} \left(\lambda \|C_k^\lambda(t)\|_{W^{n+3,4}}, \lambda^{1-\alpha} \|C_k^\lambda(t)\|_{W^{n+3,4}}^2 \right). \end{aligned}$$

To conclude, we fix some $n \in \mathbb{N}^*$ such that $n \leq r_0$ and estimate the norms of E^λ and $C_1^\lambda(0)$ on the first line thanks to assumption (2.11) and the norms of coefficient C_k^λ , $0 \leq k \leq 4$, on the second line thanks to assumption (2.12). This gives

$$(A.11) \quad \sup_{0 \leq t \leq T} \|B(t)\|_{H^n} \leq C \lambda^{1-\alpha},$$

for all $0 < \lambda < 1$ and $0 \leq n \leq r_0$, where C depends on α , on the final time T , the temperature T_0 , the size of the domain \mathbb{T} and the implicit constants in (2.11)-(2.12), and where r_0 is given in (2.11).

Using the same approach, we find the following estimates for A_1 and A_2 (defined by (A.3))

$$\sup_{0 \leq t \leq T} (\|A_1(t)\|_{W^{n,\infty}}, \|A_2(t)\|_{W^{n,\infty}}) \leq C \sup_{0 \leq t \leq T} \left(\lambda \|E^\lambda(t)\|_{W^{n+1,\infty}}, \|C_1^\lambda(0)\|_{W^{n,\infty}}, \lambda \|C_2^\lambda(0)\|_{W^{n+1,\infty}} \right).$$

We use Sobolev injections to bound the $L^\infty(\mathbb{T})$ norms with their $W^{1,4}(\mathbb{T})$ counterpart, which yields

$$\sup_{0 \leq t \leq T} (\|A_1(t)\|_{W^{n,\infty}}, \|A_2(t)\|_{W^{n,\infty}}) \leq C \sup_{0 \leq t \leq T} \left(\lambda \|E^\lambda(t)\|_{W^{n+2,4}}, \|C_1^\lambda(0)\|_{W^{n+1,4}}, \lambda \|C_2^\lambda(0)\|_{W^{n+2,4}} \right).$$

Using assumption (2.11) to estimate E^λ and C_1^λ and assumption (2.12) for C_2^λ , we find

$$(A.12) \quad \sup_{0 \leq t \leq T} (\|A_1(t)\|_{W^{n,\infty}}, \|A_2(t)\|_{W^{n,\infty}}) \leq C \lambda^{1-\alpha},$$

for all $0 < \lambda < 1$ and $0 \leq n \leq r_0$, where C depends on α , on the final time T , the temperature T_0 , the size of the domain \mathbb{T} and the implicit constants in (2.11)-(2.12), and where r_0 is given in (2.11).

Step 2. iteration of the Duhamel formula. We now focus on the iteration process. We consider some integer $l \geq 0$, take the l -th derivative in x and then the $L^2(\mathbb{T})$ -norm in (A.4). After applying Jensen inequality to bound the time integral, using that $\exp((s-t)J/\lambda)$ is an isometry of \mathbb{R}^2 and using Leibniz rule to estimate the products between A_i , $i \in \{0, 1\}$, and \mathbf{U}_1^λ , we obtain

$$\sup_{0 \leq t \leq T} \left\| \partial_x^l \mathbf{U}^\lambda(t) \right\|_{L^2} \leq C \sup_{0 \leq t \leq T} (\|A_1(t)\|_{W^{l,\infty}}, \|A_2(t)\|_{W^{l,\infty}}) \sup_{0 \leq t \leq T} \left\| \mathbf{U}_1^\lambda(t) \right\|_{H^{l+1}} + \sup_{0 \leq t \leq T} \left\| \partial_x^l B(t) \right\|_{L^2},$$

for some constant C depending on $l \geq 0$ and T . We sum the latter estimate over all integers $l \geq 0$ less than n , for any $n \in \mathbb{N}$ such that $n \leq r_0$, where r_0 is given in (2.11)

$$\sup_{0 \leq t \leq T} \left\| \mathbf{U}^\lambda(t) \right\|_{H^n} \leq C \left(\sup_{0 \leq t \leq T} (\|A_1(t)\|_{W^{n,\infty}}, \|A_2(t)\|_{W^{n,\infty}}) \sup_{0 \leq t \leq T} \left\| \mathbf{U}_1^\lambda(t) \right\|_{H^{n+1}} + \sup_{0 \leq t \leq T} \|B(t)\|_{H^n} \right),$$

for some constant C depending on $n \geq 0$ and T . We bound the norms of (A_1, A_2) according to (A.12) and the norm of B according to (A.11), which yields

$$\sup_{0 \leq t \leq T} \left\| \mathbf{U}^\lambda(t) \right\|_{H^n} \leq C \lambda^{1-\alpha} \left(\sup_{0 \leq t \leq T} \left\| \mathbf{U}_1^\lambda(t) \right\|_{H^{n+1}} + 1 \right),$$

for all $0 < \lambda < 1$ and $0 \leq n \leq r_0$, where the constant C depends on α , on the final time T , the temperature T_0 , the size of the domain \mathbb{T} and the implicit constants in (2.11)-(2.12). Next, we point out that $\|\mathbf{U}_1^\lambda\|_{H^{n+1}} \leq \|\mathbf{U}^\lambda\|_{H^{n+1}}$, which allows to iterate the latter formula with respect to n and obtain

$$\sup_{0 \leq t \leq T} \|\mathbf{U}^\lambda(t)\|_{L^2} \leq C \left(\lambda^{n(1-\alpha)} \sup_{0 \leq t \leq T} \|\mathbf{U}_1^\lambda(t)\|_{H^{n+1}} + \lambda^{1-\alpha} \right),$$

for all $0 < \lambda < 1$ and $0 \leq n \leq r_0$. Now, we fix $n = r_0$, and since $r_0 \geq 1/(1-\alpha)$, we obtain

$$\sup_{0 \leq t \leq T} \|\mathbf{U}^\lambda(t)\|_{L^2} \leq C \left(\lambda \sup_{0 \leq t \leq T} \|\mathbf{U}_1^\lambda(t)\|_{H^{r_0+1}} + \lambda^{1-\alpha} \right),$$

for all $0 < \lambda < 1$, where C depends on α , T , T_0 , \mathbb{T} and the implicit constants in (2.11)-(2.12). To bound the norm of \mathbf{U}_1^λ , we substitute \mathbf{U}_1^λ according to the following relation $\mathbf{U}_1^\lambda = E^\lambda - E_{\text{slow}}^\lambda - E_{\text{osc}}^\lambda$ and apply the triangle inequality

$$\sup_{0 \leq t \leq T} \|\mathbf{U}^\lambda(t)\|_{L^2} \leq C \left(\lambda \sup_{0 \leq t \leq T} \left(\|E^\lambda(t)\|_{H^{r_0+1}} + \|C_2^\lambda(t)\|_{H^{r_0+2}} + \|E_{\text{osc}}^\lambda(t)\|_{H^{r_0+1}} \right) + \lambda^{1-\alpha} \right).$$

To bound the norm of E_{osc}^λ , we substitute E_{osc}^λ according to (2.14) and apply the triangle inequality

$$\sup_{0 \leq t \leq T} \|\mathbf{U}^\lambda(t)\|_{L^2} \leq C \left(\sup_{0 \leq t \leq T} \left(\lambda \|E^\lambda(t)\|_{H^{r_0+1}}, \|C_1^\lambda(0)\|_{H^{r_0+1}}, \lambda \|C_2^\lambda(t)\|_{H^{r_0+2}} \right) + \lambda^{1-\alpha} \right).$$

We bound E^λ and C_1^λ thanks to (2.11) and C_2^λ thanks to (2.12), which yields the result

$$\sup_{0 \leq t \leq T} \|\mathbf{U}^\lambda(t)\|_{L^2} \leq C \lambda^{1-\alpha},$$

for all $0 < \lambda < 1$ and $0 \leq n \leq r_0$, where the constant C depends on α , on the final time T , the temperature T_0 , the size of the domain \mathbb{T} and the implicit constants in (2.11)-(2.12).

APPENDIX B. PROOF OF PROPOSITION 3.1

In this proof, we analyze the limit $\lambda \rightarrow 0$ for a fixed $\Delta t > 0$. We denote $C_k^{(1,n+1)}$ the coefficient $C_k^{(1)}$ computed in (3.4) at time step n . Our proof is divided into 2 steps. In the first one, we solve the linearized scheme (3.4) to prove that C_0^n converges to 1, that $C^{(1,n)}$ converges to 0 and that $C_2^{(1,n)}$ remains bounded uniformly in λ . In the second step, we analyze the nonlinear scheme (3.5) and use our estimate from the first step to prove that C_1^n converges to 0 and that E^n is close to $\sqrt{2} T_0 \partial_h C_2^n$ as $\lambda \rightarrow 0$.

The convergence of C_0^n is a consequence of the Poisson coupling between E^n and C_0^n . Indeed, taking the H^2 norm of the third line of (3.4) and replacing $C_0^{(1)}$ and $E^{(1)}$ with C_0^{n+1} and E^{n+1} thanks to the first two lines in (3.5), we deduce

$$\|C_0^{n+1} - 1\|_{h^2(\mathcal{J})} = \lambda^2 \|E^{n+1}\|_{h^3(\mathcal{J})},$$

for all $0 \leq n+1 \leq T/\Delta t$. The latter relation is also valid when $n+1 = 0$. Hence, we bound the right hand side according to (3.8), which yields for all $\lambda > 0$

$$(B.1) \quad \sup_{0 \leq n \leq T/\Delta t} \|C_0^n - 1\|_{h^2(\mathcal{J})} \leq C \lambda.$$

To demonstrate that $(C_1^{(1,n)})_{1 \leq n \leq T/\Delta t}$ converges, we take the H^2 norm in the second line of (3.4) with $k = 0$, which yields

$$\sqrt{T_0} \left\| \partial_h C_1^{(1,n+1)} \right\|_{h^2(\mathcal{J})} = \left\| \frac{C_0^{(1,n+1)} - C_0^n}{\Delta t} \right\|_{h^2(\mathcal{J})}.$$

We take the supremum over all $1 \leq n+1 \leq T/\Delta t$ in the latter relation and bound the right hand side according to the first line in (B.1), which gives

$$(B.2) \quad \sup_{1 \leq n \leq T/\Delta t} \left\| \partial_h C_1^{(1,n)} \right\|_{h^2(\mathcal{J})} \leq C \lambda \quad \forall \lambda > 0,$$

where the constant $C > 0$ depends on Δt . To control the full H^3 norm of C_1 , we bound the L^2 norm of C_1 with the L^2 norms of $\partial_h C_1$ thanks to a discrete Poincaré-Wirtinger inequality [5, Lemma 3.3], which reads

$$\|C_1^n\|_{l^2(\mathcal{J})} \leq C \|\partial_h C_1^n\|_{l^2(\mathcal{J})} + C \left| \sum_{j \in \mathcal{J}} C_{1,j}^n \Delta x_j \right|.$$

We check that the total flux on the right hand side is 0 thanks to assumption (3.7) and standard computation, that is,

$$\sum_{j \in \mathcal{J}} C_{1,j}^n \Delta x_j = \sum_{j \in \mathcal{J}} C_{1,j}^{(1,n+1)} \Delta x_j = 0,$$

for all $n \geq 0$. Therefore, we obtain

$$(B.3) \quad \|C_1^n\|_{l^2(\mathcal{J})} \leq C \|\partial_h C_1^n\|_{l^2(\mathcal{J})}, \quad \text{and} \quad \|C_1^{(1,n+1)}\|_{l^2(\mathcal{J})} \leq C \|\partial_h C_1^{(1,n+1)}\|_{l^2(\mathcal{J})}.$$

Together with (B.2), the last inequality yields

$$(B.4) \quad \sup_{1 \leq n \leq T/\Delta t} \|C_1^{(1,n)}\|_{h^3(\mathcal{J})} \leq C\lambda, \quad \forall \lambda > 0.$$

Next, we show that $C_2^{(1,n)}$ is bounded for all $1 \leq n \leq T/\Delta t$. To do so, we take the discrete derivative ∂_h^r , where $0 \leq r \leq 2$, of the second line of (3.4), multiply it by $\partial_h^r C_k^{(1,n+1)}$ and sum over all $k \in \{2, \dots, N_H\}$. After a discrete integration by part with respect to $j \in \mathcal{J}$, this yields

$$\sum_{k=2}^{N_H} \|\partial_h^r C_k^{(1,n+1)}\|_{l^2(\mathcal{J})}^2 \leq \Delta t \sqrt{2T_0} \|\partial_h^{r+1} C_1^{(1,n+1)}\|_{l^2(\mathcal{J})} \|\partial_h^r C_2^{(1,n+1)}\|_{l^2(\mathcal{J})} + \sum_{k=2}^{N_H} \|\partial_h^r C_k^n\|_{l^2(\mathcal{J})}^2.$$

We bound $C_1^{(1,n+1)}$ on the right hand side according to (B.4) and we estimate the sum thanks to assumption (3.9). This yields

$$\|\partial_h^r C_2^{(1,n+1)}\|_{l^2(\mathcal{J})}^2 \leq C \left(\|\partial_h^r C_2^{(1,n+1)}\|_{l^2(\mathcal{J})} + 1 \right).$$

Hence, we deduce that for all $\lambda > 0$, it holds

$$(B.5) \quad \sup_{1 \leq n \leq T/\Delta t} \|C_2^{(1,n)}\|_{h^2(\mathcal{J})} \leq C.$$

The last step consists in proving that C_1^n is of order λ for all $1 \leq n \leq T/\Delta t$ and that E^n is close to $\sqrt{2}T_0 \partial_h C_2^n$ for all $2 \leq n \leq T/\Delta t$ as $\lambda \rightarrow 0$. We proceed in three steps:

- we first prove that E^n is uniformly bounded in λ for all $1 \leq n \leq T/\Delta t$;
- we deduce that C_1^n is of order λ for all $1 \leq n \leq T/\Delta t$;
- we obtain that E^n is close to $\sqrt{2}T_0 \partial_h C_2^n$ for all $2 \leq n \leq T/\Delta t$ as $\lambda \rightarrow 0$.

Let us first prove that E^n is uniformly bounded in λ for all $n \geq 1$. We take the H^1 norm in the first line of (3.4), which yields

$$\|E^{(1,n+1)}\|_{h^1(\mathcal{J})} \leq \sqrt{2}T_0 \|\partial_h C_2^{(1,n+1)}\|_{h^1(\mathcal{J})} + \frac{\sqrt{T_0}}{\Delta t} \left(\|C_1^{(1,n+1)}\|_{h^1(\mathcal{J})} + \|C_1^n\|_{h^1(\mathcal{J})} \right) + T_0 \|\partial_h C_0^{(1,n+1)}\|_{h^1(\mathcal{J})}.$$

On the right hand side, we estimate C_0 according to (B.1), $C_1^{(1,n+1)}$ according to (B.4), $C_2^{(1,n+1)}$ according to (B.5) and assumption (3.8) to estimate C_1^n . We obtain that for all $\lambda > 0$, it holds

$$(B.6) \quad \sup_{1 \leq n \leq T/\Delta t} \|E^n\|_{h^1(\mathcal{J})} \leq C.$$

Next, we deduce that C_1^n is of order λ for all $1 \leq n \leq T/\Delta t$. To do so, we take the L^2 norm of the derivative of (3.5) with $k = 1$, which yields

$$\|\partial_h C_1^{n+1}\|_{l^2(\mathcal{J})} \leq \|\partial_h C_1^{(1,n+1)}\|_{l^2(\mathcal{J})} + \frac{\Delta t}{\sqrt{T_0}} \|\partial_h (E^{n+1} (C_0^{n+1} - 1))\|_{l^2(\mathcal{J})}.$$

We estimate $C_1^{(1,n+1)}$ thanks to (B.4), which gives

$$\|\partial_h C_1^{n+1}\|_{l^2(\mathcal{J})} \leq C \left(\|\partial_h (E^{n+1} (C_0^{n+1} - 1))\|_{l^2(\mathcal{J})} + \lambda \right).$$

We estimate the derivative of the product between E^{n+1} and $C_0^{n+1} - 1$, as follows

$$\|\partial_h C_1^{n+1}\|_{l^2(\mathcal{J})} \leq C \left(\|E^{n+1}\|_{l^\infty(\mathcal{J})} \|C_0^{n+1} - 1\|_{h^1(\mathcal{J})} + \|E^{n+1}\|_{h^1(\mathcal{J})} \|C_0^{n+1} - 1\|_{l^\infty(\mathcal{J})} + \lambda \right).$$

To estimate the L^∞ norms, we use the following Sobolev inequality, which holds true in dimension 1 and under assumption (3.10)

$$(B.7) \quad \|E^{n+1}\|_{l^\infty(\mathcal{J})} \leq C \|E^{n+1}\|_{h^1(\mathcal{J})}.$$

We deduce

$$\|\partial_h C_1^{n+1}\|_{l^2(\mathcal{J})} \leq C \left(\|E^{n+1}\|_{h^1(\mathcal{J})} \|C_0^{n+1} - 1\|_{h^1(\mathcal{J})} + \lambda \right).$$

We estimate the norm of E^{n+1} thanks to (B.6), the norm of $C_0^{n+1} - 1$ thanks to (B.1) and take the supremum over all $1 \leq n+1 \leq T/\Delta t$, we find

$$\sup_{1 \leq n \leq T/\Delta t} \|\partial_h C_1^n\|_{l^2(\mathcal{J})} \leq C\lambda, \quad \forall \lambda > 0.$$

To control the full H^1 norm of C_1^n , we apply the discrete Poincaré inequality (B.3), which yields the first estimate in (3.11)

$$(B.8) \quad \sup_{1 \leq n \leq T/\Delta t} \|C_1^n\|_{h^1(\mathcal{J})} \leq C\lambda, \quad \forall \lambda > 0.$$

To conclude, we prove that E^n is close to $\sqrt{2}T_0 \partial_h C_2^n$ for all $2 \leq n \leq T/\Delta t$ as $\lambda \rightarrow 0$. To do so, we take the L^2 norm in the first line of (3.4), which yields

$$\|E^{(1,n+1)} - \sqrt{2}T_0 \partial_h C_2^{(1,n+1)}\|_{l^2(\mathcal{J})} \leq \frac{\sqrt{T_0}}{\Delta t} \left(\|C_1^{(1,n+1)}\|_{l^2(\mathcal{J})} + \|C_1^n\|_{l^2(\mathcal{J})} \right) + T_0 \|\partial_h C_0^{(1,n+1)}\|_{l^2(\mathcal{J})}.$$

On the right hand side, we estimate C_0 according to (B.1), $C_1^{(1,n+1)}$ according to (B.4), and C_1^n according to the latter estimate in (B.8), which yields

$$(B.9) \quad \|E^{n+1} - \sqrt{2}T_0 \partial_h C_2^{(1,n+1)}\|_{l^2(\mathcal{J})} \leq C\lambda,$$

for all $n \geq 1$. Then, we prove that $\partial_h C_2^{(1,n+1)}$ is close to $\partial_h C_2^{n+1}$ taking the L^2 norm in (3.5) with $k = 2$, which yields

$$\|\partial_h (C_2^{n+1} - C_2^{(1,n+1)})\|_{l^2(\mathcal{J})} \leq C \|\partial_h (E^{n+1} C_1^{n+1})\|_{l^2(\mathcal{J})}$$

We estimate the derivative of the product $\partial_h (E^{n+1} C_1^{n+1})$ as follows

$$\|\partial_h (C_2^{n+1} - C_2^{(1,n+1)})\|_{l^2(\mathcal{J})} \leq C \left(\|E^{n+1}\|_{l^\infty(\mathcal{J})} \|\partial_h C_1^{n+1}\|_{l^2(\mathcal{J})} + \|\partial_h E^{n+1}\|_{l^2(\mathcal{J})} \|C_1^{n+1}\|_{l^\infty(\mathcal{J})} \right).$$

Then, we apply the Sobolev inequality (B.7) to estimate the L^∞ norms in the last inequality and deduce

$$\|\partial_h (C_2^{n+1} - C_2^{(1,n+1)})\|_{l^2(\mathcal{J})} \leq C \|E^{n+1}\|_{h^1(\mathcal{J})} \|C_1^{n+1}\|_{h^1(\mathcal{J})}.$$

We estimate the norm of E^{n+1} thanks to (B.6) and the norm of C_1^{n+1} thanks to (B.8), which yields

$$\|\partial_h (C_2^{n+1} - C_2^{(1,n+1)})\|_{l^2(\mathcal{J})} \leq C\lambda,$$

for all $n \geq 1$. Plugging the latter estimate in (B.9) and taking the supremum over all $1 \leq n \leq T/\Delta t - 1$, we deduce the result the second estimate in (3.11)

$$\sup_{2 \leq n \leq T/\Delta t} \|E^n - \sqrt{2}T_0 \partial_h C_2^n\|_{l^2(\mathcal{J})} \leq C\lambda, \quad \forall \lambda > 0,$$

which concludes the proof.

APPENDIX C. PROOF OF PROPOSITION 3.3

Using (3.4) and (3.5), the equations for C_0^{n+1} , C_1^{n+1} and E^{n+1} can be re-written

$$(C.1) \quad \begin{cases} \frac{C_0^{n+1} - C_0^n}{\Delta t} + \sqrt{T_0} \partial_h \left(C_1^{n+1} - \Delta t \frac{1}{\sqrt{T_0}} E^{n+1} (C_0^{n+1} - 1) \right) = 0, \\ \frac{C_1^{n+1} - C_1^n}{\Delta t} + \sqrt{T_0} \partial_h C_0^{n+1} + \sqrt{2T_0} \partial_h C_2^{(1,n+1)} - \frac{1}{\sqrt{T_0}} E^{n+1} C_0^{n+1} = 0, \\ \lambda^2 \partial_h E^{n+1} = C_0^{n+1} - 1, \end{cases}$$

where $C_2^{(1,n+1)}$ corresponds to $C_2^{(1)}$ calculated during the Step 1 of the calculus of $(C_k^{n+1})_{k \geq 0}$ knowing $(C_k^n)_{k \geq 0}$.

Then, inserting the first equation of (C.1) into the third one, we get

$$\begin{aligned} \lambda^2 \frac{\partial_h E^{n+1} - 2 \partial_h E^n + \partial_h E^{n-1}}{\Delta t^2} &= \frac{C_0^{n+1} - 2 C_0^n + C_0^{n-1}}{\Delta t^2} \\ &= -\sqrt{T_0} \frac{\partial_h C_1^{n+1} - \partial_h C_1^n}{\Delta t} + \partial_h \left(E^{n+1} (C_0^{n+1} - 1) - E^n (C_0^n - 1) \right). \end{aligned}$$

Now, using the second and third equations of (C.1) yields

$$\begin{aligned} \lambda^2 \frac{\partial_h E^{n+1} - 2 \partial_h E^n + \partial_h E^{n-1}}{\Delta t^2} &= \partial_h^2 \left(\sqrt{2} T_0 C_2^{(1,n+1)} + T_0 C_0^{n+1} \right) - \partial_h \left(E^{n+1} C_0^{n+1} \right) + \lambda^2 \partial_h \left(E^{n+1} \partial_h E^{n+1} - E^n \partial_h E^n \right). \end{aligned}$$

REFERENCES

- [1] K. R. Arun, N. Crouseilles, and S. Samantaray. High order asymptotic preserving and classical semi-implicit RK schemes for the Euler-Poisson system in the quasineutral limit. *J. Sci. Comput.*, 100(1):Paper No. 24, 34, 2024.
- [2] C. Bardos. About a variant of the 1d Vlasov equation, dubbed “Vlasov-Dirac-Benney equation”. In *Séminaire Laurent Schwartz-Équations aux dérivées partielles et applications*. École Polytech., Palaiseau, 2012-2013.
- [3] R. Belaouar, N. Crouseilles, P. Degond, and E. Sonnendrücker. An asymptotically stable semi-Lagrangian scheme in the quasi-neutral limit. *J. Sci. Comput.*, 41(3):341–365, 2009.
- [4] A. Blaustein. Structure preserving solver for Multi-dimensional Vlasov-Poisson type equations. working paper or preprint, Feb. 2024.
- [5] A. Blaustein and F. Filbet. On a discrete framework of hypocoercivity for kinetic equations. *Math. Comp.*, 93(345):163–202, 2024.
- [6] A. Blaustein and F. Filbet. A structure and asymptotic preserving scheme for the Vlasov-Poisson-Fokker-Planck model. *J. Comput. Phys.*, 498:Paper No. 112693, 25, 2024.
- [7] A. Bobylev and I. Potapenko. On solutions of Vlasov-Poisson-Landau equations for slowly varying in space initial data. *Kinet. Relat. Models*, 16(1):20–40, 2023.
- [8] A. V. Bobylev and I. F. Potapenko. Long wave asymptotics for the Vlasov-Poisson-Landau kinetic equation. *J. Stat. Phys.*, 175(1):1–18, 2019.
- [9] S. Boscarino, F. Filbet, and G. Russo. High order semi-implicit schemes for time dependent partial differential equations. *Journal of Scientific Computing*, 68:975–1001, 2016.
- [10] Y. Brenier. Convergence of the Vlasov-Poisson system to the incompressible Euler equations. *Comm. Partial Differential Equations*, 25(3-4):737–754, 2000.
- [11] R. Caflisch, C. Wang, G. Dimarco, B. Cohen, and A. Dimits. A hybrid method for accelerated simulation of Coulomb collisions in a plasma. *Multiscale Model. Simul.*, 7(2):865–887, 2008.
- [12] F. F. Chen. *Introduction to plasma physics and controlled fusion*, volume 1. Springer, 1984.
- [13] P. Crispel, P. Degond, and M.-H. Vignal. An asymptotic preserving scheme for the two-fluid Euler-Poisson model in the quasineutral limit. *J. Comput. Phys.*, 223(1):208–234, 2007.
- [14] N. Crouseilles, G. Dimarco, and M.-H. Vignal. Multiscale schemes for the BGK-Vlasov-Poisson system in the quasi-neutral and fluid limits. Stability analysis and first order schemes. *Multiscale Model. Simul.*, 14(1):65–95, 2016.
- [15] P. Degond. Asymptotic-preserving schemes for fluid models of plasmas. In *Numerical models for fusion*, volume 39/40 of *Panor. Synthèses*, pages 1–90. Soc. Math. France, Paris, 2013.
- [16] P. Degond and F. Deluzet. Asymptotic-preserving methods and multiscale models for plasma physics. *J. Comput. Phys.*, 336:429–457, 2017.
- [17] P. Degond, F. Deluzet, and D. Doyen. Asymptotic-preserving particle-in-cell methods for the Vlasov-Maxwell system in the quasi-neutral limit. *J. Comput. Phys.*, 330:467–492, 2017.
- [18] P. Degond, F. Deluzet, L. Navoret, A.-B. Sun, and M.-H. Vignal. Asymptotic-preserving particle-in-cell method for the Vlasov-Poisson system near quasineutrality. *J. Comput. Phys.*, 229(16):5630–5652, 2010.
- [19] P. Degond, J.-G. Liu, and M.-H. Vignal. Analysis of an asymptotic preserving scheme for the Euler-Poisson system in the quasineutral limit. *SIAM Journal on Numerical Analysis*, 46(3):1298–1322, 2008.

- [20] G. Dimarco, L. Mieussens, and V. Rispoli. An asymptotic preserving automatic domain decomposition method for the Vlasov-Poisson-BGK system with applications to plasmas. *J. Comput. Phys.*, 274:122–139, 2014.
- [21] F. Filbet and S. Jin. A class of asymptotic-preserving schemes for kinetic equations and related problems with stiff sources. *J. Comput. Phys.*, 229(20):7625–7648, 2010.
- [22] F. Filbet and T. Rey. A hierarchy of hybrid numerical methods for multiscale kinetic equations. *SIAM J. Sci. Comput.*, 37(3):A1218–A1247, 2015.
- [23] F. Filbet and T. Xiong. A hybrid discontinuous Galerkin scheme for multi-scale kinetic equations. *J. Comput. Phys.*, 372:841–863, 2018.
- [24] D. Gérard-Varet, D. Han-Kwan, and F. Rousset. Quasineutral limit of the Euler-Poisson system for ions in a domain with boundaries II. *J. Éc. polytech. Math.*, 1:343–386, 2014.
- [25] E. Grenier. Oscillations in quasineutral plasmas. *Comm. Partial Differential Equations*, 21(3-4):363–394, 1996.
- [26] M. Griffin-Pickering and M. Iacobelli. Recent developments on quasineutral limits for Vlasov-type equations. In *Recent advances in kinetic equations and applications*, volume 48 of *Springer INdAM Ser.*, pages 211–231. Springer, 2021.
- [27] D. Han-Kwan and M. Hauray. Stability issues in the quasineutral limit of the one-dimensional Vlasov-Poisson equation. *Comm. Math. Phys.*, 334(2):1101–1152, 2015.
- [28] D. Han-Kwan and M. Iacobelli. Quasineutral limit for Vlasov-Poisson via Wasserstein stability estimates in higher dimension. *J. Differential Equations*, 263(1):1–25, 2017.
- [29] D. Han-Kwan and F. Rousset. Quasineutral limit for Vlasov-Poisson with Penrose stable data. *Ann. Sci. Éc. Norm. Supér. (4)*, 49(6):1445–1495, 2016.
- [30] L. Ji, Z. Yang, Z. Li, D. Wu, S. Jin, and Z. Xu. An asymptotic-preserving and energy-conserving particle-in-cell method for Vlasov-Maxwell equations. *J. Math. Phys.*, 64(6):Paper No. 063503, 19, 2023.
- [31] S. Jin. Efficient asymptotic-preserving (AP) schemes for some multiscale kinetic equations. *SIAM J. Sci. Comput.*, 21(2):441–454, 1999.
- [32] S. Jin. Asymptotic-preserving schemes for multiscale physical problems. *Acta Numer.*, 31:415–489, 2022.
- [33] H. Liu, X. Cai, Y. Cao, and G. Lapenta. An asymptotic-preserving conservative semi-Lagrangian scheme for the Vlasov-Maxwell system in the quasi-neutral limit. *J. Comput. Phys.*, 528:Paper No. 113840, 2025.
- [34] L. Pareschi and G. Russo. Implicit–explicit Runge–Kutta schemes and applications to hyperbolic systems with relaxation. *Journal of Scientific computing*, 25:129–155, 2005.